



1 **Inter-annual variation of aerosol pollution in East Asia and**  
2 **its relation with strong/weak East Asian winter monsoon**

3 Min Xie <sup>1\*</sup>, Lei Shu <sup>1</sup>, Ti-jian Wang <sup>1\*</sup>, Da Gao <sup>1</sup>, Shu Li <sup>1</sup>, Bing-liang Zhuang <sup>1</sup>, Anning Huang <sup>1</sup>,  
4 Dexian Fang <sup>2</sup>, Yong Han <sup>1</sup>, Mengmeng Li <sup>1</sup>, Pu-long Chen <sup>1</sup>, Zhi-jun Liu <sup>1</sup>, Zheng Wu <sup>2</sup>, Hua Lu <sup>2</sup>

5 <sup>1</sup> School of Atmospheric Sciences, CMA-NJU Joint Laboratory for Climate Prediction Studies,  
6 Jiangsu Collaborative Innovation Center for Climate Change, Nanjing University, Nanjing 210023,  
7 China

8 <sup>2</sup> Chongqing Institute of Meteorology and Science, Chongqing 401147, China

9 -----  
10 \* Corresponding authors. School of Atmospheric Sciences, Nanjing University, Nanjing 210023,  
11 China. [minxie@nju.edu.cn](mailto:minxie@nju.edu.cn) (M. Xie), [tjwang@nju.edu.cn](mailto:tjwang@nju.edu.cn) (T. J. Wang)

12  
13 **Abstract:** Aerosol has become one of the major air pollutants in East Asia, and its spatial  
14 distribution can be affected by the East Asian monsoon circulation. By means of the observational  
15 analysis and the numerical simulation, the inter-annual variation of wintertime aerosol pollution in  
16 East Asia and its association with strong/weak East Asian winter monsoon (EAWM) are  
17 investigated in this study. Firstly, the Moderate Resolution Imaging Spectroradiometer/Aerosol  
18 Optical Depth (MODIS/AOD) records during 2000-2013 are analyzed to reveal the inter-annual  
19 variation characteristics of aerosols. It is found that there is an increasing trend of AOD in East  
20 Asia over the last decade, implying the increasing aerosol loading in this region. The areas with  
21 obvious increasing AOD cover the Sichuan Basin (SCB), the North China Plain, and most of the  
22 Middle-Lower Yangtze River Plain in China. Secondly, the EAWM index (EAWMI) based on the  
23 characteristic of circulation are calculated to investigate the inter-annual variations of EAWM. The  
24 National Centers for Environmental Prediction (NCEP) reanalysis data are used in EAWMI  
25 calculation and meteorological analysis. Nine strong and thirteen weak EAWM years are  
26 identified from 1979 to 2014. In these strong EAWM years, the sea-land pressure contrast  
27 increases, the East Asian trough strengthens, and the northerly wind gets anomalous over East  
28 Asia. More cold air masses are forced to move southward by strengthened wind field and make  
29 cool. In the weak EAWM years, however, the situation is totally on the opposite. Finally, the



30 effects of strong/weak EAWM on the distribution of aerosols in East Asia are discussed. It is  
31 found that the northerly wind strengthens (weakens) and transports more (less) aerosols southward  
32 in strong (weak) EAWM years, resulting in higher (lower) AOD in the north and lower (higher)  
33 AOD in the south. The long-term weakening trend of EAWM may potentially increase the aerosol  
34 loading. Apart from the changes in aerosol emissions, the weakening of EAWM should be another  
35 cause that results in the increase of AOD over the Yangtze River Delta (YRD) region, the  
36 Beijing-Tianjin-Hebei (BTH) region and SCB but the decrease of AOD over the Pearl River Delta  
37 (PRD) region. Using the Regional Climate-Chemistry coupled Model System (RegCCMS), we  
38 further prove that the intensity of EAWM has great impacts on the spatial distribution of aerosols.  
39 In strong (weak) EAWM years, there is a negative (positive) anomaly in the air column content of  
40 aerosol, with a reduction (increment) of  $-80$  ( $25$ )  $\text{mg}\cdot\text{m}^{-2}$ . The change pattern of aerosol  
41 concentrations in lower troposphere is different from that at 500 hPa, which is related with the  
42 different change pattern of meteorological fields in EAWM circulation at different altitude. More  
43 obvious changes occur in lower atmosphere, the change pattern of aerosol column content in  
44 different EAWM years is mainly decided by the change of aerosols in lower troposphere.

45 **Key words:** East Asian winter monsoon; Monsoon index; Aerosol; AOD; RegCCMS

46

## 47 1. Introduction

48 Atmospheric aerosol refers to the particulate matter in solid or liquid phase suspended in the  
49 atmosphere with a diameter between  $0.001$ - $100$   $\mu\text{m}$ . It is not only a significant atmospheric  
50 pollutant (Zhang et al., 2012b; 2013; Ding et al., 2013; 2016; Zhao et al., 2013; Guo et al., 2014;  
51 Quan et al., 2014; Zheng et al., 2015), but also an important climate forcing factor that can directly  
52 or indirectly affect the earth climate by influencing atmospheric radiation (Twomey, 1977;  
53 Ramanathan et al., 2001a; Nakajima et al., 2003; Li, et al., 2007), air temperature (Albrecht, 1989;  
54 Giorgi et al., 2003; Liu et al., 2016), cloud physics (Fan et al., 2012; 2013; Nair et al., 2012),  
55 precipitation (Rosenfeld, 2000; Rosenfeld et al., 2008; Giorgi et al., 2003; Qian et al., 2009;  
56 Konwar et al., 2012), wind (Jacobson and Kaufman, 2006; Bollasina et al., 2011; 2014; ; Yang et  
57 al., 2013), and atmospheric circulation (Allen et al., 2014; Niu et al., 2010; Song et al., 2014) etc.  
58 On the other hand, changes of meteorological conditions (temperature, precipitation, and monsoon  
59 circulation etc.) also can influence the emission, transport, chemical reaction and deposition



60 processes of aerosols, and thereby worsen the air quality (Jacob and Winner, 2009; Isaksen et al.,  
61 2009; von Schneidmesser, 2015; Wu et al., 2016; Xie et al., 2017). For the above-mentioned  
62 reasons, the relationship between aerosol pollution and climate system is acquired worldwide  
63 attention in the scientific community (Isaksen et al., 2009; von Schneidmesser, 2015; Wu et al.,  
64 2016; Li et al., 2016c). In the past decade, the interactions between aerosol and monsoon climate  
65 has become the hot topic (Li et al., 2016c), especially in South Asia (Ramanathan et al., 2001a;  
66 2001b; Ganguly et al., 2012; Nair et al., 2012; Manoj et al., 2012; Bollasina et al., 2011; 2014) and  
67 East Asia (Nakajima et al., 2003; Lau et al., 2006; Li et al., 2007; 2009; 2016a; 2016b; Niu et al.,  
68 2010; Zhang et al., 2010; 2012b; 2013; 2014; Zhao et al., 2010; 2013; Yan et al., 2011; Zhu et al.,  
69 2012; Mu and Zhang, 2014; Song et al., 2014; Chen and Wang, 2015; Wang et al., 2015; Wu et al.,  
70 2016).

71 East Asia is one of the most densely populous regions, and the homeland of one-third of the  
72 world population (Li et al., 2011). In the past decades, the rapid development of economy,  
73 industry and agriculture with expanding population in East Asia has resulted in large amounts of  
74 anthropogenic aerosol emissions in this region (Li et al., 2016c). It was reported that the aerosol  
75 concentration in East Asia (especially eastern China) is second to that of the cities in South Asia,  
76 and the anthropogenic components (sulfate, nitrate and organics, etc.) account for a large  
77 proportion of total aerosols (Zhang et al., 2008; 2012b; 2013). This high level of aerosol pollution  
78 can exert much influence on regional atmospheric environment (Ding et al., 2013; 2016; Xie et al.,  
79 2016; Zhu et al., 2017), weather (Ding et al., 2013; 2016) and climate (Nakajima et al., 2003; Lau  
80 et al., 2006; Zhuang et al., 2013a; 2013b; Song et al., 2014; Wang et al., 2015; Li et al., 2007;  
81 2009; 2011; 2016b). On the other hand, East Asia experiences the most remarkable monsoon  
82 climate. The variation in monsoon circulation can not only directly affect the climatic  
83 characteristics (air temperature, precipitation, and atmospheric circulation etc.), but also affect the  
84 horizontal and vertical transport of atmospheric matters, such as moisture (Zhang, 2001; Fu et al.,  
85 2006), cloud droplet (Tang et al., 2014), and air pollutants (Liu et al., 2003; Randel et al., 2010;  
86 Bian et al., 2011) etc. Thus, the production, emission, transport and deposition processes of  
87 aerosols can be significantly impacted by the East Asian monsoon circulation (Niu et al., 2010;  
88 Zhang et al., 2010; 2013; 2014; Zhao et al., 2010; 2013; Yan et al., 2011; Zhu et al., 2012; Mu and  
89 Zhang, 2014; Chen and Wang, 2015; Li et al., 2016a; 2016b; 2016c; Wu et al., 2016).



90           There have been lots of studies concerning the interactions between aerosol and monsoon  
91 climate over East Asia. Some considered the mechanisms of the aerosol impact on monsoon  
92 climate (Nakajima et al., 2003; Lau et al., 2006; Li et al., 2011; 2016b; Manoj et al., 2012; Song et  
93 al., 2014; Wang et al., 2015). Some tried to reveal the effects of monsoon climate on aerosols (Niu  
94 et al., 2010; Zhang et al., 2010; 2013; 2014; Zhao et al., 2010; 2013; Liu et al., 2011; Yan et al.,  
95 2011; Zhu et al., 2012; Chen and Wang, 2015; Wang et al., 2015; Li et al., 2016a). However,  
96 many of the previous studies about the later topic mainly focused on the impacts of summer  
97 monsoon climate (Zhang et al., 2010; Zhao et al., 2010; Liu et al., 2011; Yan et al., 2011; Zhu et  
98 al., 2012; Wang et al., 2015; Li et al., 2016c; Wu et al., 2016). In East Asia, high aerosol pollution  
99 episodes usually occur in winter. Thus, how the East Asian winter monsoon (EAWM) circulation  
100 modulates aerosols is worth to be investigated, and can help us comprehensively understand the  
101 formation of aerosol pollution over East Asia in recent years.

102           Some researchers have gained improved knowledge of the effect of EAWM on aerosol  
103 pollution (Mu and Zhang, 2014). For example, Zhao et al. (2013) and Zhang et al. (2013) pointed  
104 out that the high concentration of local aerosols in North China can weaken the incoming  
105 solar radiation on the ground, increase the atmospheric stratification stability, and in turn cause the  
106 continuously and cumulatively increase of aerosols. Besides, the outward transport of aerosols is  
107 weakened by the weak monsoon circulation in the winter, which also helps to cause the  
108 continuous fog and haze weather in China. Zhang et al. (2014) analyzed the meteorological  
109 conditions during the severe fog-haze periods over eastern China in January 2013. They concluded  
110 that with weak winter monsoon circulation, the upper westerly jet slows down, vertical shear in  
111 horizontal winds recedes, and thereby the development of synoptic disturbances and the vertical  
112 mixing of the air masses are weakened. These anomalies in meteorology are all favorable for the  
113 maintenance and the development of fog-haze over eastern China. Meanwhile, the anomaly of  
114 south wind in the lower and middle level of troposphere hinders the outward transport of aerosols  
115 as well. From these studies, it was found that the aerosol pollution episodes are inextricably linked  
116 with the weak monsoon circulation, but the conclusion was just on basis of the individual aerosol  
117 pollution episodes.

118           Several researchers have tried to understand the effect of EAWM on aerosol pollution in East  
119 Asia by exploring the long-term variation trends of air pollutants and climate (Niu et al., 2010;



120 Chen and Wang, 2015; Li et al., 2016a). Based on the records of thirty years, Niu et al. (2010)  
121 found that the frequencies of wintertime fog-haze events have doubled across eastern-central  
122 China, while the speed of surface wind and the frequency of cold wave respectively decreased by  
123 19% and 29% for the same period. They pointed out that weakening of the EAWM is likely a  
124 major cause for the changes in meteorology, and has potential impact on the enhancing aerosol  
125 loading and wintertime fog in China (Niu et al., 2010). However, they did not emphasize the  
126 inter-annual variation of EAWM and aerosol, and could not reveal the exact different effects of  
127 strong and weak EAWM on aerosols. Chen and Wang (2015) investigated haze days in North  
128 China as well as the associated atmospheric circulations during 1960–2012, and mentioned that  
129 the weakened northerly winds, the inversion anomalies in the lower troposphere, the weakened  
130 East Asian trough in the midtroposphere, and the northward East Asian jet in the high troposphere  
131 are the main causes leading to the winter haze. But, they studied the variation and the driving  
132 factors in all seasons only based on the observation data of visibility. Special attention should be  
133 paid to winter, and model simulation should be applied to probe the exact mechanism of the  
134 EAWM impact on aerosols. Li et al. (2016a) investigated the inter-annual variation of wintertime  
135 fog-haze events over eastern-central China from 1972 to 2014 and its association with EAWM.  
136 They revealed that the stronger (weaker) the EAWM is, the less (more) the fog-haze events occur.  
137 This phenomenon is related with the changes of near-surface winds, vertical shear in horizontal  
138 winds, and divergence or convergence in the upper troposphere in different EAWM years (Li et al.,  
139 2016a). However, this work was only based on the observational analysis of meteorological data,  
140 and did not exactly present how EAWM impacts the distribution of aerosols. To better reveal the  
141 mechanisms of the EAWM impact on aerosol, the inter-annual variation of EAWM, as well as the  
142 difference in aerosol distribution in different EAWM years, should be discussed, and integrated  
143 approach based on long-term observations and improved models is needed to further analyze the  
144 mechanism (Li et al., 2016c).

145 The main purpose of this study is to improve our understanding of the effects of circulation  
146 variation of EAWM on the distribution and transport of aerosols. By means of the observational  
147 analysis of the Moderate Resolution Imaging Spectroradiometer/Aerosol Optical Depth  
148 (MODIS/AOD) records and the National Centers for Environmental Prediction (NCEP) reanalysis  
149 data during 2000-2013, as well as the Regional Climate-Chemistry coupled Model System



150 (RegCCMS) numerical simulation, we focus on (1) the long-term variation trend of aerosols in the  
151 wintertime of East Asia, (2) the inter-annual variation of EAWM by identifying the strong/weak  
152 EAWM years based on a EAWM index (EAWMI), and (3) the effects of strong/weak EAWM on  
153 the distribution of aerosols. In this paper, detailed descriptions about the observational records for  
154 aerosol and meteorology, the method to calculate EAWMI, and the adopted model with  
155 configuration are illustrated in Section 2. The main findings, including the inter-annual variations  
156 of AOD and EAWM, as well as the effect of EAWM on the distribution of aerosols in the winter  
157 of East Asia, are given in Section 3. In the end, a brief summary is presented in Section 4.

158

## 159 **2. Data and methods**

### 160 **2.1 Aerosol optical depth records and meteorological data**

161 The MODIS/AOD monthly records from 2000 to 2013 are used to analysis the distribution  
162 characteristic of aerosols in the winter of East Asia, and its inter-annual variation in the past  
163 decade. The data can be collected from MODIS Collection 5.1 dataset, with wave band of 550 nm  
164 and a horizontal resolution of  $1^\circ \times 1^\circ$ . Much work has been done to validate the feasibility of  
165 MODIS aerosol products, and it was found that MODIS/AOD has reached the designed accuracy  
166 with an error within  $\pm 0.05 \sim \pm 0.20 \tau$  (Chu et al., 2002). The application of MODIS products in  
167 China presents great territorial and seasonal differences, but the applicability of the products  
168 reaches above 80% in the area with homogeneous surface and high-covered vegetation, which can  
169 meet the error standard ( $>70\%$ ) of NASA (Wang et al., 2007). In general, the satisfying accuracy,  
170 the high spatial resolution, and the high temporal coverage of MODIS/AOD make it widely  
171 applied in scientific research for the regional distribution of aerosols (Tao et al., 2013; Li and Han,  
172 2016).

173 In this study, the meteorological data are used to calculate the East Asian winter monsoon  
174 index (EAWMI) that is used to identify the intensity of EAWM, and analyze the changes of  
175 meteorological factors in the strong/weak EAWM years. The data are obtained from the NECP  
176 global monthly reanalysis data from 2000 to 2013, including the large-scale meteorological  
177 variables such as geopotential height, air temperature, zonal wind, meridional wind, sea level  
178 pressure and precipitation etc., with a horizontal resolution of  $2.5^\circ \times 2.5^\circ$  and a vertical resolution  
179 of 17 levels. December, as well as January and February in the following year, is regarded as the



180 winter months.

## 181 **2.2 East Asian winter monsoon index**

182 EAWM is a complex atmospheric circulation system, the strength of which is affected by  
183 diverse factors. The appropriate monsoon index is of great significance to explore the variation of  
184 EAWM. There are lots of indices measuring the intensity of EAWM applied in previous studies.  
185 They are mainly classified into 5 classes, which are on basis of the characteristic of circulation, the  
186 characteristic of wind field, the characteristic of high pressure, the characteristic of sea-land  
187 pressure contrast, and the integrated characteristic of winter monsoon system, respectively (Shao  
188 and Li, 2012). According to their different research focuses of EAWM, these indices differ from  
189 each other in the definition of monsoon intensity. The previous comparison showed that EAWMI  
190 calculated by the characteristic of circulation or wind field can identify the strong/weak EAWM  
191 better than other monsoon indices, and thereby these two kinds of indices (especially the first one)  
192 have been widely applied in relevant studies (Shao and Li, 2012). Consequently, we choose the  
193 EAWM index based on the characteristic of circulation to describe the anomaly of EAWM in this  
194 work.

195 The EAWM originates from the periodic southward movement of the strong northeast air  
196 stream in the front of the Siberian High. Thus, in terms of the circulation situation, the intensity of  
197 EAWM can be manifested as the variations of the intensity of the East Asian trough at 500 hPa  
198 and the Mongolia high near the surface. In this case, the activity of the East Asian trough at 500  
199 hPa can be used to represent the state of EAWM (Yan et al., 2004; Wang and He, 2012). Based on  
200 the work of Yan et al. (2004), the monthly averaged geopotential heights at 500 hPa in December,  
201 January and February is firstly standardized. Then the average value covering the area of  
202 (30°–45°N, 125°–145°E) is calculated as follows:

$$203 \quad \bar{H} = H_{500}(25 - 40^{\circ}N, 110 - 130^{\circ}E) \quad (1)$$

204 where,  $\bar{H}$  is the average of geopotential heights at 500 hPa ( $H_{500}$ ). Finally,  $\bar{H}$  is standardized to  
205 be the value between -1 and 1, as the following algorithm:

$$206 \quad EAWMI = \frac{(\bar{H}_i - \mu)}{\sigma} \quad (2)$$

207 where,  $\bar{H}_i$ ,  $\mu$  and  $\sigma$  are the value to be standardized, the mean value and the standard deviation of



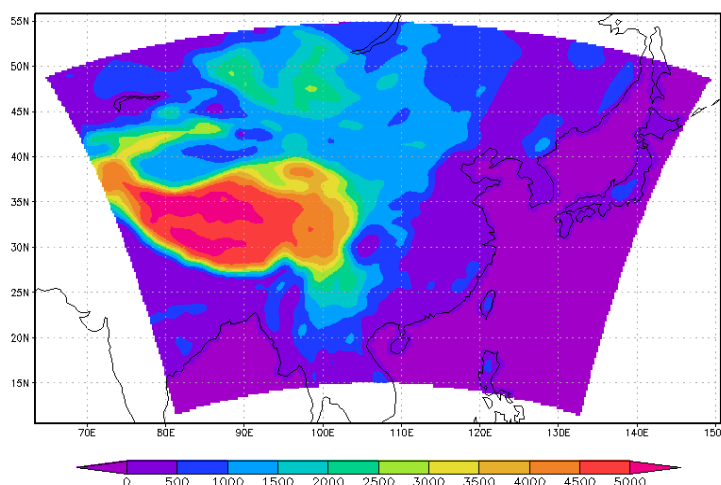
208 all sample points, respectively. EAWMI is the EAWM index used in this study. Previous  
209 researches have proved that it can well demonstrate the characteristics of circulation and air  
210 temperature in East Asia (Yan et al., 2004; Shao and Li, 2012).

### 211 **2.3 Regional climate chemistry modeling system and its simulation configuration**

212 The regional climate chemistry modeling system (RegCCMS) used in this study is an on-line  
213 coupled model system composed of Regional Climate Model (RegCM3) with Tropospheric  
214 Atmospheric Chemistry Model (TACM) (Li et al., 2009; Zhuang et al., 2013a; 2013b; Wang et al.,  
215 2010; 2015). RegCM3 was developed by International Center for Theoretical Physics Research  
216 Center (ICTP) in Trieste, Italy (Pal et al., 2007). Its dynamical core is based on the hydrostatic  
217 version of the fifth generation Pennsylvania State University–National Center for Atmospheric  
218 Research (PSU–NCAR) mesoscale model MM5. It adopts the terrain-following sigma coordinate,  
219 and its radiation scheme takes the effects of greenhouse gases, aerosols, and ice clouds into  
220 consideration (Giorgi et al., 2003; 2004a; 2004b). TACM includes complicated atmospheric  
221 chemical and physical processes to deal with the emissions, transports, transformations and  
222 depositions of trace gases and aerosols (Zhuang et al., 2013a; 2013b), and can be applied to  
223 simulate the effects of primary pollutant emissions (eg., SO<sub>2</sub>, NO<sub>x</sub> and VOCs etc.) on the regional  
224 pollution of gases, aerosols, and acid deposition (Wang et al., 2010; 2015). RegCM3 and TACM  
225 are two-way coupled in RegCCMS. RegCM3 provides meteorological data to drive TACM,  
226 including air temperature and solar radiation data used in the calculation of chemical reaction rates,  
227 cloud cover and actinic flux data used in the calculation of photolysis rate, moisture data needed in  
228 some atmospheric chemistry reactions, wind field and turbulent field required to deal with the  
229 advection, diffusion and dry deposition processes of pollutants, and cloud and rainfall parameters  
230 required to deal with liquid phase chemical and wet scavenging processes. On the other hand,  
231 TACM outputs the spatial and vertical distributions of trace gases and aerosols, some of which  
232 have special influence on atmospheric radiation transfer and can affect the radiation process in  
233 RegCM3. Numerous previous studies have shown that RegCCMS have a satisfying performance  
234 in the simulations of climate change and air quality. It can better simulate the regional  
235 meteorological fields, the concentrations of air pollutants, and the climatic effects of various  
236 aerosols, including black carbon, nitrate, sulfate, and primary organic carbon (Li et al., 2009;  
237 Wang et al., 2010; 2015; Zhuang et al., 2013a; 2013b).



238 RegCCMS is applied in this study to simulate the differences in meteorological field and  
239 aerosol distribution between strong and weak EAWM years, and further reveal the effects of  
240 EAWM on the transport and the distribution of aerosols over East Asia. Figure 1 shows the grid  
241 setting of the simulated domain, which covers most of East Asia, with the center point at 34.5°N,  
242 116.8°E, horizontal grids of  $121 \times 90$ , and grid spacing of 50 km. From the surface to the model  
243 top (50 hPa), there are 18 vertical sigma layers, with the  $\sigma$  values of 1.0, 0.99, 0.98, 0.96, 0.93,  
244 0.89, 0.84, 0.78, 0.71, 0.63, 0.55, 0.47, 0.39, 0.31, 0.23, 0.16, 0.1, 0.05 and 0.0.  
245



246  
247 **Figure 1. The grid setting of the simulated domain in RegCCMS.**

248  
249 The major selected physical options in RegCM3 include the ACM2 boundary layer scheme  
250 (Holtslag and Boville, 1990), the CCM3 radiation scheme (Kiehl et al., 1996), the BATS  
251 land-surface scheme (Dickinson, 1993), the Grell cumulus parameterization scheme (Grell and  
252 Devenyi, 2002). The initial and boundary conditions of meteorological fields are obtained from  
253 NCEP global reanalysis data with  $2.5^\circ \times 2.5^\circ$  resolution.

254 For TACM, the finite positive definite difference method of Smolarkiewicz for the advective  
255 term (Smolarkiewicz, 1984), the Crank-Nicolson scheme for the vertical diffusion term, and the  
256 central difference scheme for the horizontal diffusion term (Press et al., 1992) are used. As for the  
257 chemical options, a condensed gas-phase chemistry scheme, a simple aqueous chemistry scheme,  
258 and the aerosol model ISORROPIA are adopted. The gas-phase chemistry scheme includes 20



259 species and 36 reactions (Wang et al., 2010). The aqueous chemistry scheme considers the soluble  
260 gases absorbed by cloud and rain droplets as well as the aqueous oxidation of SO<sub>2</sub> and NO<sub>x</sub> (Wang  
261 et al., 2010). ISORROPIA is a thermodynamic equilibrium model that can simulate sulfate and  
262 nitrate aerosols (Nenes et al., 1998). The resistance analogy method named the big leaf model  
263 (Walmsley and Wesely, 1996) is used to simulate dry deposition velocities. The in-cloud and  
264 below-cloud scavenging of aerosols are calculated as a function of rainfall amount (Wang et al.,  
265 2010). More details of the schemes can be found in the previous studies (Li et al., 2009; Wang et  
266 al., 2010; 2015; Zhuang et al., 2013a; 2013b). The emission inventory used in this study is based  
267 on the work of Zhuang et al. (2013a; 2013b) and Wang et al. (2015). It is basically obtained from  
268 the inventory that is developed for the NASA INTEX-B mission (Zhang et al., 2009), and includes  
269 the emissions of aerosols and associated precursors over China in 2006 with the monthly  
270 variations of pollutants.

271

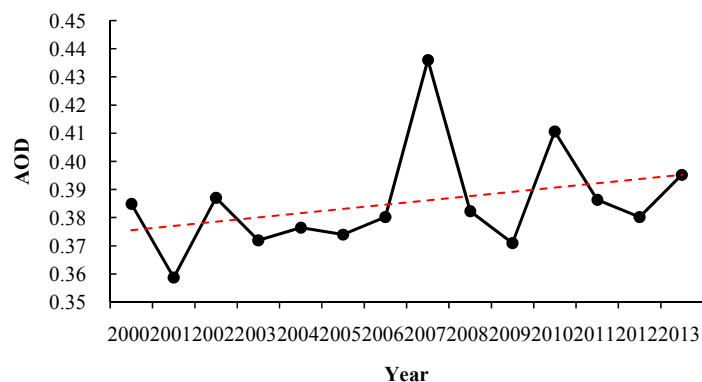
### 272 **3. Influence of EAWM on the distribution of aerosols based on observational analysis**

#### 273 **3.1 Characteristic of the inter-annual variation of wintertime aerosols in East Asia**

274 Figure 2 shows the time series of average wintertime AOD in East Asia from 2000 to 2013.  
275 From the linear trend (red dotted line in Figure 2), it is clear that the pollution level of aerosols in  
276 East Asia gets significantly increased in the past ten years, which should be mainly caused by the  
277 increased emissions of aerosols associated with the rapid development of economy over East Asia  
278 in these years (Zhang et al., 2012b). In addition, some previous studies also revealed that the  
279 increasingly aerosol loading may be tightly related to the weakening of EAWM during the same  
280 period (Niu et al., 2010; Li et al., 2016a). Figure 2 shows the obvious inter-annual variation of the  
281 wintertime AOD from 2000 to 2013 as well, with the maximum mean value of 0.44 in 2007 and  
282 the minimum value of 0.36 in 2001. This suggests that the anomalous monsoon circulation may  
283 play great roles in the inter-annual variation of aerosol loading in this region, which is further  
284 discussed in Section 3.4 in detail.

285

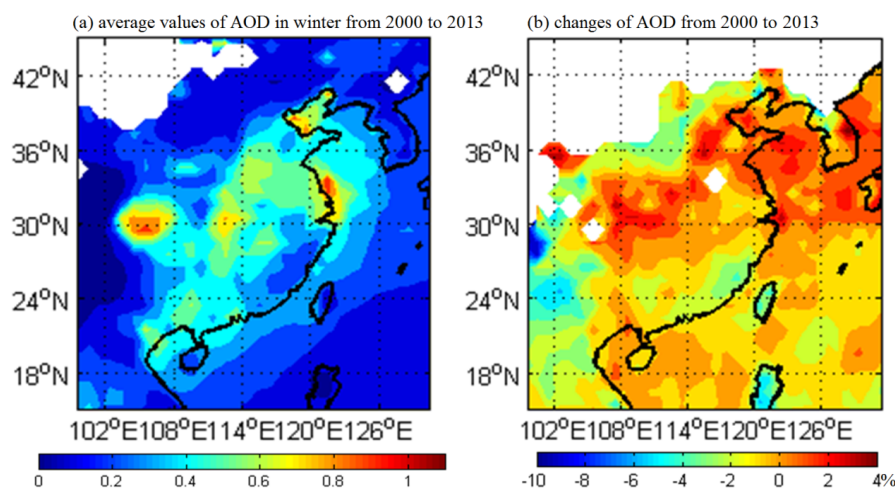
286



287  
288 **Figure 2. Inter-annual variation (black solid line) and linear trend (red dotted line) of AOD in the winter of**  
289 **East Asia from 2000 to 2013.**

290

291 The spatial distributions of the average value (Figure 3a) and the changes (Figure 3b) of  
292 wintertime AOD over East Asia during the period of 2000-2013 are demonstrated in Figure 3. As  
293 shown in Figure 3a, the spatial distribution of AOD shows a clear regional feature over East Asia.  
294 Although the values of AOD differ in different months, the areas with high AOD value are mainly  
295 concentrated in the Sichuan Basin (SCB), around Bohai Bay, and in the Middle-Lower reaches of  
296 Yangtze River in China. Meantime, from Figure 3b, it is found that the wintertime AOD over East  
297 Asia shows a long-term rising trend, with a significantly increase in North China, Central China,  
298 SCB and the Yangtze River Delta (YRD) region. To sum up, the areas with heavy aerosol loading  
299 in East Asia mainly consist of the Beijing-Tianjin-Hebei (BTH) region (115-120°E, 35-41°N),  
300 YRD (117-122°E, 30-34°N), and SCB (103-107°E, 28-32°N). Besides, the Pearl River Delta (PRD)  
301 region (111-116°E, 18-24°N) is a remarkable developed urban agglomeration in South China, and  
302 its aerosol pollution can represent the level of fog-haze pollution in the south of East Asia.



303

304 **Figure 3.** The spatial distribution of the average value and the changes of AOD over East Asia during the  
305 period of winter 2000-2013.

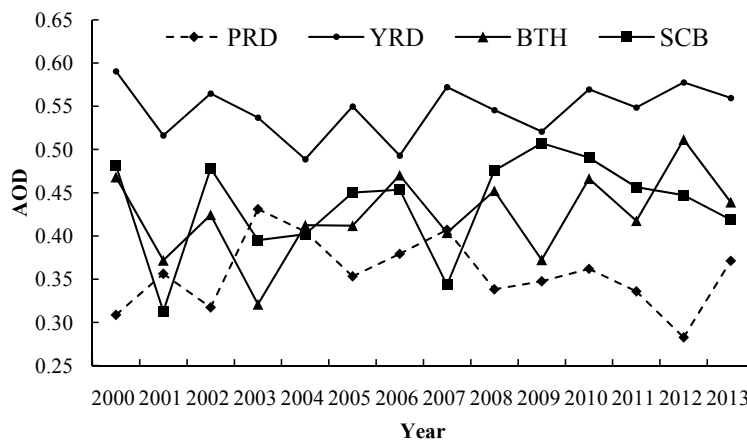
306

307 Figure 4 presents the inter-annual variation of average wintertime AOD in the above four  
308 typical regions of East Asia from 2000 to 2013. The following Table 1 gives the corresponding  
309 statistics. It can be seen that the value of AOD in YRD is much higher than that in other regions,  
310 with the average, maximum and minimum value being 0.55, 0.59 (in 2000) and 0.48 (in 2004),  
311 respectively. As for other three regions, the respective average, maximum and minimum AOD  
312 values are 0.44, 0.51 (in 2012) and 0.31 (in 2003) for SCB, 0.42, 0.51 (in 2012) and 0.32 (in 2003)  
313 for BTH, and 0.36, 0.43 (in 2003) and 0.28 (in 2012) for PRD. Except for PRD, the AOD values  
314 in other three regions show a rising trend. As shown in Figure 4 and Table 1, the largest ten-year  
315 increment is 13.1% in BTH, followed by 9.4% in SCB and 2.4% in YRD. Based on the satellite  
316 remote sensing data, it was found that there exists the largest increase of air pollutant  
317 concentrations in BTH and YRD during the last ten years, which has caused the increase of  
318 particulate matter concentrations in these two regions (Zhang et al., 2012a). Increased emissions  
319 produced by human activities have resulted in the increase of AOD and haze weather in SCB, and  
320 the special topography of basin can also lead to the aggravation of fog-haze pollution in this  
321 region to a certain extent because of the constraint effect of topography on the transport and  
322 diffusion of aerosols (Chen et al., 2014). As for the PRD region, there is a slight reduction in AOD  
323 during recent years with the reduction of -3.6%, which may be mainly attributed to the scientific



324 and effective control of air quality in this region for a long time.

325



326

327 **Figure 4. Average value of wintertime AOD in the four typical regions from 2000 to 2013.**

328

329 **Table 1. Statistics values of wintertime AOD in the four typical regions during the period of 2000-2013.**

	Maximum	Minimum	Average	10-year increment
BTH	0.51	0.32	0.42	13.1%
YRD	0.59	0.49	0.55	2.4%
SCB	0.51	0.31	0.44	9.4%
PRD	0.43	0.28	0.36	-3.6%

330

### 331 3.2 Inter-annual variation of EAWM

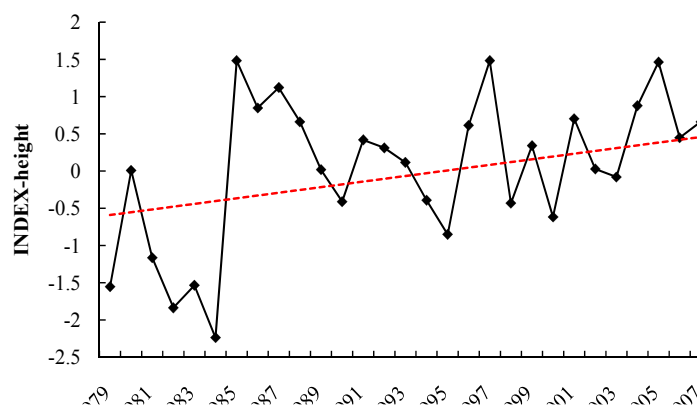
332 Figure 5 shows the inter-annual variation of EAWMI from 1979 to 2014. According to the  
 333 definition of EAWMI in Section 2.2, when EAWMI is larger than 0, the positive anomaly of 500  
 334 hPa geopotential height occurs over East Asia (25~40°N, 110~130°E). In this case, the East Asian  
 335 trough is shallow, and its upper northwest air stream is comparatively weak. Thus, there is a weak  
 336 winter monsoon circulation in East Asia, which tends to result in weak cold air activities. On the  
 337 contrary, when EAWMI is lower than 0, there is a deeper East Asian trough that is related with a  
 338 stronger upper northwest air stream. The stronger cold air activities frequently take place, and  
 339 thereby result in the stronger winter monsoon. Thus, the value of EAWMI in a year can be used as  
 340 the criterion to distinguish if the year is a weak or strong winter monsoon year.

341 From the linear variation depicted in Figure 5, the value of EAWMI shows an increasing  
 342 trend, with the value larger than 0.5 and even above 1 in recent years. The trend means that the



343 East Asian winter monsoon circulation has been significantly weakened during recent decades.  
344 Moreover, the comparison of Figure 5 and Figure 3 further implies that the weakened winter  
345 monsoon may increase the wintertime AOD loading over East Asia, which is in agreement with  
346 the findings of Xu et al. (2006), Niu et al. (2010) and Li et al. (2016a).

347 As shown in Figure 5, the EAWMI also presents a strong inter-annual variation, with the  
348 maximum value of 1.5, the minimum value of -2.2 and the maximum inter-annual difference of  
349 3.7. According to the definition of Wang and Chen (2014), the year with the value of  
350 EAWMI  $>0.5$  ( $<-0.5$ ) is identified to be the weak (strong) EAWM year. Consequently, there are 9  
351 strong EAWM years (1979, 1980, 1982-1985, 1996, 2001 and 2010) and 13 weak EAWM years  
352 (1986-1989, 1997, 1998, 2002, 2005-2006, 2008 and 2012-2014) being identified from 1979 to  
353 2014. Obviously, there are more strong EAWM years before 1986, with the lowest value of  
354 EAWMI being -2.2 in 1985. After 1986, EAWM tends to be weaker, and there are more weak  
355 EAWM years instead. This conclusion corresponds to the previous findings (Nakamura et al.,  
356 2002; Jhun and Lee, 2004; Wang et al., 2009).



357  
358 **Figure 5. Inter-annual variation of EAWMI from 1979 to 2014.**  
359

### 360 **3.3 Difference in meteorological fields between strong and weak EAWM years**

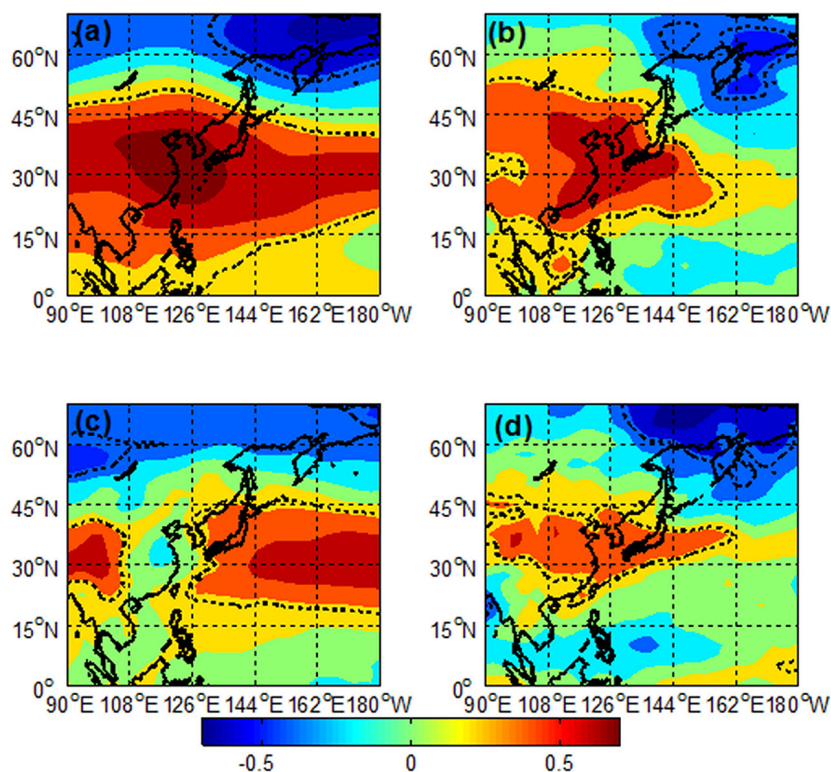
361 The EAWMI used in this study can well illustrate the variation of circulation resulting from  
362 the EAWM anomaly. Figure 6 presents the spatial distribution of correlation coefficient between  
363 EAWMI and some meteorological factors over East Asia. As shown in the figure, there exists a  
364 distinct positive correlation between EAWMI and 500 hPa geopotential height (Figure 6a), surface  
365 temperature (Figure 6a), precipitation (Figure 6c), and sea level pressure (Figure 6d) in most area



366 of (20~40°N, 108~135°E), with the largest correlation coefficient being 0.8, 0.8, 0.6 and 0.8,  
367 respectively.

368 For the correlation between EAWMI and 500 hPa geopotential height, it seems that the  
369 increase in the value of EAWMI corresponds to the shallow 500 hPa East Asian trough, the less  
370 cold air activity, and the weak EAWM circulation. Under this circumstance, the surface air  
371 temperature gets increased (Figure 6b), implying that the surface temperature in weak EAWM  
372 years is higher than that in strong EAWM years. As mentioned in other researches, this EAWMI  
373 indeed can reflect the anomaly of average winter temperature over East Asia to some extent (Yan  
374 et al., 2004; Shao and Li, 2012). With respect to the correlation between EAWMI and sea level  
375 pressure, it is found that the thermal low over the west Pacific Ocean strengthens as the increased  
376 EAWMI (Figure 6c). Generally, there are a cold high on the land and a thermal low on the sea in  
377 the winter of East Asia. Thus, the positive correlation in Figure 6c also means that the sea-land  
378 pressure contrast decreases in weak EAWM years while it increases in strong EAWM years. When  
379 it comes to precipitation (Figure 6d), it increases when the value of EAWMI rises up. It can be  
380 concluded that there is more rainfall in weak EAWM years than in normal years over East Asian  
381 continent. On the contrary, the East Asian continent features a dry cold climate with low surface  
382 temperature in strong EAWM years. Overall, it is convinced that the EAWMI can reflect the  
383 variation anomaly of 500 hPa geopotential height, surface temperature, sea-level pressure and  
384 precipitation over East Asian continent to some extent.

385



386

387 **Figure 6. The correlation coefficient between EAWMI and meteorological factors, including (a) 500 hPa**  
388 **geopotential height, (b) surface temperature, (c) sea-level pressure and (d) precipitation.**

389

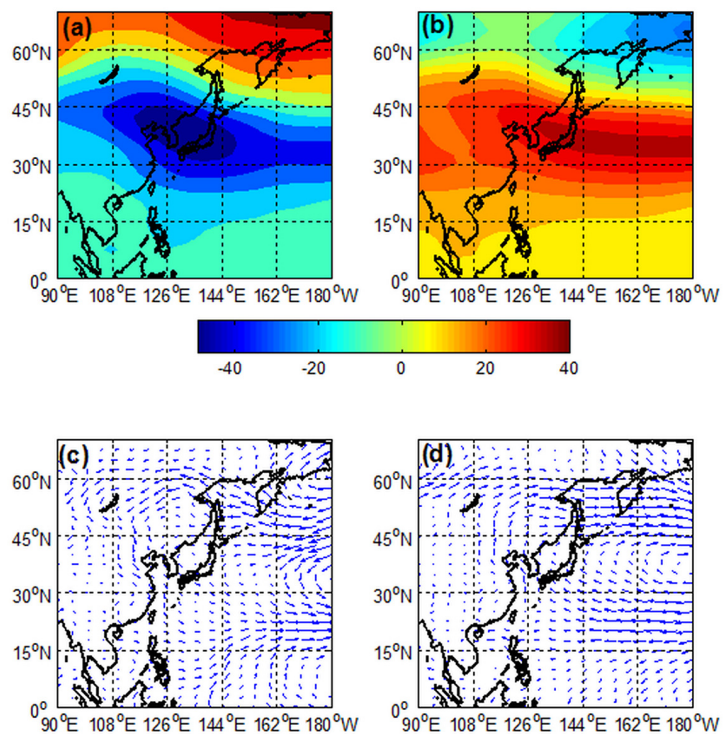
390 The differences in meteorological factors between strong and weak EAWM years are  
391 examined, targeted at the 9 strong and the 13 weak EAWM years mentioned in Section 3.2. Figure  
392 7 shows the average anomaly of the meteorological factors in the strong and the weak EAWM  
393 years. Apparently, the spatial distributions of circulation and meteorological factors in the strong  
394 EAWM years are almost completely opposite to those in the weak EAWM years. Figure 7a and b  
395 demonstrate the anomaly of 500 hPa geopotential height field in different EAWM years. In the  
396 strong EAWM years (Figure 7a), there are a negative anomaly in the East Asian trough and a  
397 positive anomaly in high latitude area of East Asia, which can be in favor of the deepening and  
398 strengthening of the East Asian trough. However, in the weak EAWM years (Figure 7b), there is a  
399 positive anomaly in the core area of the East Asian trough, making the trough shallower and  
400 weaker. Figure 7c and d present the wind field anomaly at the 850 hPa level in different EAWM  
401 years. It seems that the north wind anomaly prevails at 850 hPa over East Asia, and the northwest



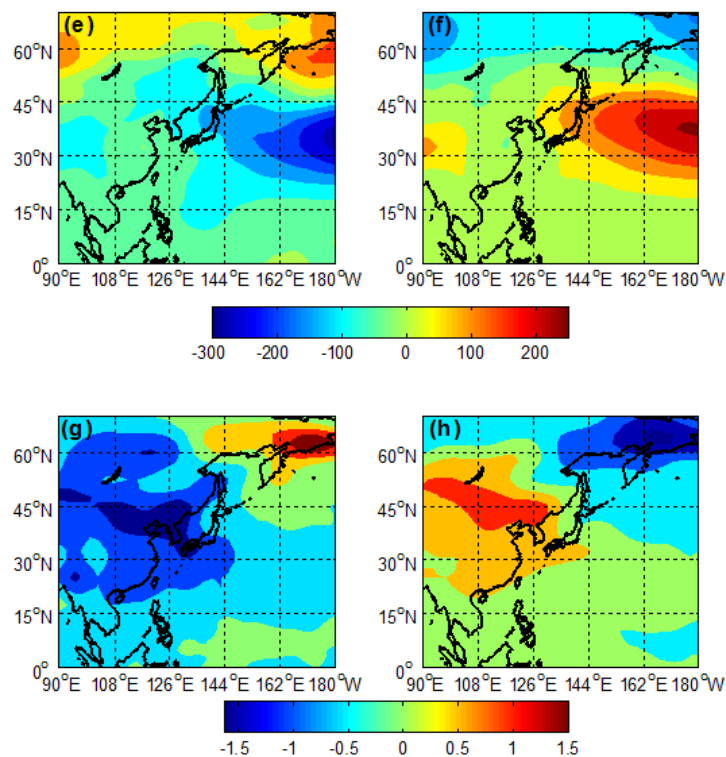
402 and the north wind dominate over the east of China in the strong EAWM years (Figure 7c).  
403 Meanwhile, there also exists a west wind anomaly near 20°N and an east wind anomaly near 50°N  
404 in North Pacific Ocean. But as shown in Figure 7d, the 850 hPa wind field in the weak EAWM  
405 years is contrary to that in the strong EAWM years. These findings are in agreement with the  
406 results obtained from Yan (2004). For the anomaly of the sea-level pressure field, Figure 7e  
407 illustrates that there is a negative anomaly of sea-level pressure in the strong EAWM years. The  
408 sea-level pressure is lower in these years than in normal years, which means that there are larger  
409 sea-land pressure contrast and stronger winter monsoon circulation in strong EAWM years.  
410 However, Figure 7f presents the different pattern in the weak EAWM years, that is, the sea-land  
411 pressure contrast is smaller and the winter monsoon circulation is generally weaker. Figure 7g and  
412 h provide the surface air temperature anomaly. It is clearly observed that there is a negative  
413 anomaly of the average winter temperature in the mainland of China in the strong EAWM years  
414 (Figure 7g). The drop of air temperature should be related with the fact that more cold air masses  
415 may be transported from north to south (Figure 7c). In the weak EAWM years, the opposite  
416 conditions appear (Figure 7h).

417 On the whole, the anomaly of atmospheric circulation in the strong EAWM years can be  
418 characterized as: (1) there is a positive anomaly in the Siberian High, a negative anomaly in  
419 sea-level pressure over Pacific Ocean area, and an apparent increase of sea-land pressure contrast;  
420 (2) there is an obvious anomaly of cyclonic circulation in 850 hPa wind field over East Asia, and  
421 thereby the northerly wind prevails over East China; (3) the 500 hPa geopotential height gets  
422 decreased over East Asia and increased over the Pacific Ocean area, which synthetically lead to  
423 the strengthening of the East Asian trough; (4) there is stronger north wind in northeast and north  
424 China, which allows more cold air mass to invade northward and results in a sharp fall in air  
425 temperature in most of East Asia. The anomalies of the meteorological factors in the weak EAWM  
426 years are almost completely opposite to the above characteristics.

427



428



429  
430 **Figure 7.** Anomaly of meteorological factors in strong EAWM years (a, c, e and g) and weak EAWM years (b,  
431 d, f and h), including (a-b) 500 hPa geopotential height (unit: m), (c-d) 850hPa wind field, (e-f) sea-level  
432 pressure (unit: Pa) and (g-h) surface air temperature (unit: °C).

433

#### 434 **3.4 Difference of aerosol distribution between strong and weak EAWM Years**

435 The spatial distribution of aerosols is not only highly connected to the local anthropogenic  
436 emissions, but also to the long-range transport influenced by atmospheric circulation and the  
437 scavenging effects of rainfall. Given that East Asia is located in the famous monsoon climate  
438 region, we analyze the difference of the distribution of aerosols between strong and weak EAWM  
439 years, aimed to figure out the effects of EAWM on aerosol pollution in this region. Only the  
440 MODIS/AOD data after 2000 are available in this study, so the data in 2 strong EAWM years  
441 (2001 and 2010) and 4 weak EAWM years (2002, 2005, 2006 and 2008) are used in this section to  
442 conduct composite analysis.

443 Figure 8a and b display the wintertime average distribution of AOD over East Asia in the  
444 above-mentioned strong and weak EAWM years. Admittedly, the regions with high AOD in the  
445 strong and the weak EAWM years are generally unchanged, and mainly concentrated in the



446 well-developed areas of East China, such as those around Bohai Bay, the North China Plain, and  
447 the Middle-Lower reaches of Yangtze River. It indicates that the anthropogenic emissions are  
448 mainly responsible for the high values of AOD instead of the winter monsoon circulation. Figure  
449 8c shows the difference of AOD distribution between the strong EAWM years and the normal  
450 years (that is anomaly), while Figure 8d illustrates that between the weak EAWM years and the  
451 normal years. In strong EAWM years, the aerosol loading is lower in the northern area of East  
452 Asia and slightly higher in the southern area than that of normal years (Figure 8c). Thereinto, there  
453 are obvious negative anomalies in North China, SCB and the middle reach of Yangtze River,  
454 implying that aerosols get decreased in these areas. But in the weak EAWM years, there are  
455 positive anomalies in these three regions, which may be attributed to the increase of aerosol  
456 concentrations. Meanwhile, there are negative anomalies in most of southern China, suggesting  
457 that the aerosol loading decreases and is lower than that of normal years.

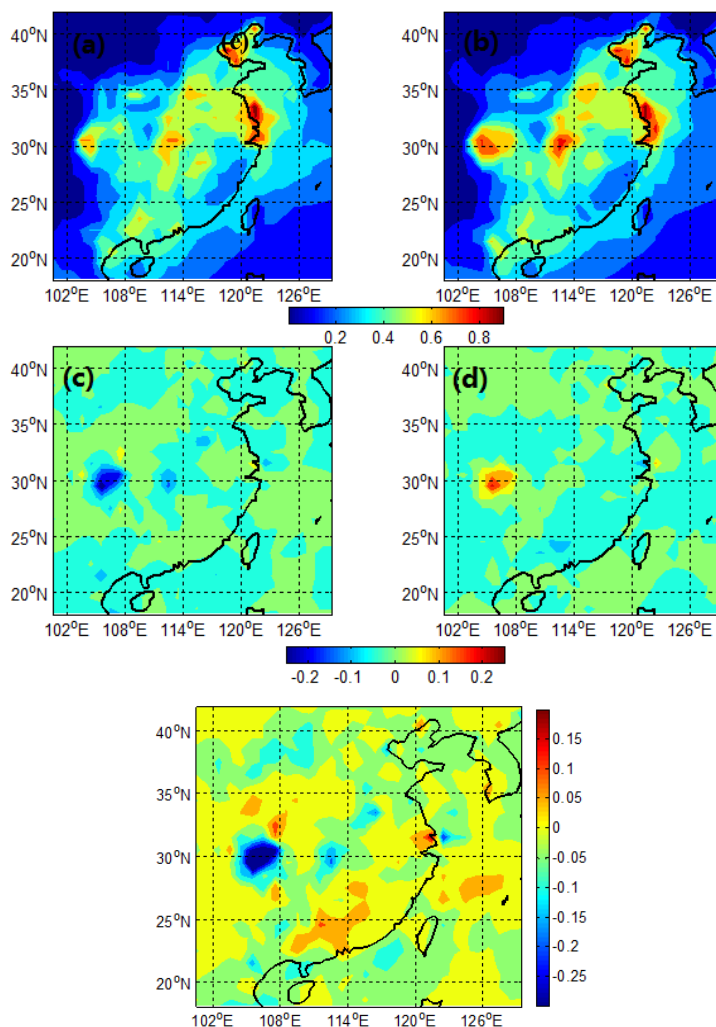
458 Figure 8e further displays the differences of aerosol distribution between the strong and the  
459 weak EAWM years, by means of subtracting from AOD in the weak EAWM years from that in the  
460 strong EAWM years. The difference distinctly reveals that there are fewer aerosols over North  
461 China, SCB, and the middle reach of Yangtze River while more aerosols over the south of East  
462 Asia in the strong EAWM years than in the weak EAWM years (Figure 8e). The difference can be  
463 explained by the prevailing wind over East Asia. In the strong EAWM years, there is a prevailing  
464 northerly wind, which can transport more aerosols in the north to the south area of East Asia. In  
465 the weak EAWM years, however, the wind is not strong, and more pollutants may be trapped and  
466 accumulated in the north because of the stagnant weather condition.

467 On account that the East Asian winter monsoon circulation tends to be weakened in the past  
468 decades (as shown in Figure 5), the weak of EAWM should be another cause that results in the  
469 increase of AOD over YRD, BTH and SCB but the decrease of AOD over PRD during this period  
470 (as shown in Figure 4). As discussed in Section 3.3, the weakening of EAWM circulation is highly  
471 related with the weakening of the East Asian trough and the Siberian High, the reduction of the  
472 sea-land pressure contrast over Pacific Ocean area, and the decrease of the northerly wind over  
473 East China. Thus, the weather tends to be more stagnant in recent years, and thereby more aerosols  
474 remain and lead to higher AOD values in the source areas (such as YRD, BTH and SCB). In  
475 winter, more pollutants are emitted from the surface in the north because of more heating demands,



476 so the aerosol pollution in the north is generally worse than that in the south. The decrease of the  
477 northerly wind results in the decrease of transport of aerosols from the north to the south, which  
478 may contribute to the decrease of the AOD value in PRD.

479



480

481

482 **Figure 8.** Composite analysis of AOD, including average AOD distribution in the strong (a) and the weak (b)  
483 EAWM years, the anomaly of the distribution of AOD in the strong (c) and the weak (d) EAWM years, and  
484 (e) difference of AOD distribution between the strong and the weak EAWM years. Here, the strong EAWM  
485 years include 2001 and 2010, while the weak EAWM years include 2002, 2005, 2006 and 2008.

486

#### 487 4. Simulation of the effects of EAWM on aerosol distribution

488

To reveal the possible impacts of EAWM on the transport and the distribution of aerosols, the



489 regional climate chemical model RegCCMS is used to model the concentrations of aerosols in the  
490 strong and the weak EAWM years. The simulations are conducted for every winter from 2001 to  
491 2010. The emissions are assumed to remain fixed in different years to eliminate the influence of  
492 emission changes. The model outputs are averaged to represent the mean distribution of aerosols  
493 over the last 10 years, the strong EAWM years (2001 and 2010), and the weak EAWM years  
494 (2002, 2005, 2006 and 2008). Because the emissions keep fixed, the differences of the distribution  
495 of aerosols between the strong EAWM years and the weak EAWM years can be considered to be  
496 only caused by the anomaly of the EAWM circulation. Other simulation settings are listed in  
497 Section 2.3.

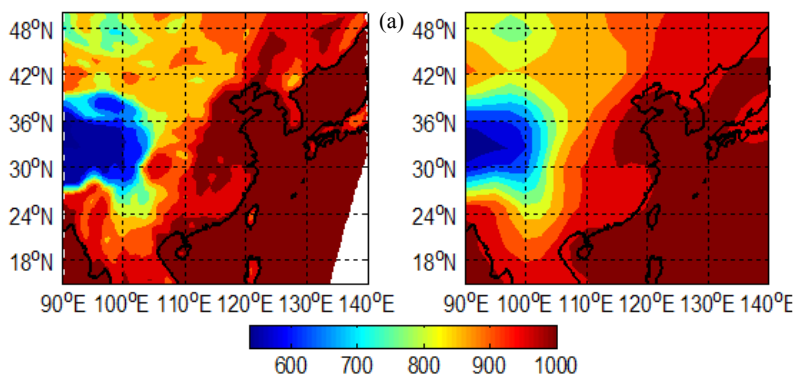
#### 498 **4.1 Model validation**

499 In order to evaluate the model performance, the NCEP reanalysis data is adopted to verify the  
500 accuracy and applicability of the modeling results from RegCCMS. Figure 9 shows the  
501 comparisons between the reanalysis data and the model results in winter (December, January and  
502 February) for the multi-year mean (from 2001 to 2010) values of surface air pressure, temperature  
503 and wind field at 850 hPa, air temperature at 500 hPa. It is certain that the results from RegCCMS  
504 simulations are consistent with those from the NCEP reanalysis data. The best performance can be  
505 found in the simulations for the surface air pressure (Figure 9a). The simulated high and low  
506 values of surface air pressure, as well as the spatial distribution, match well with the reanalysis  
507 data. The simulated air temperature fields at 850 hPa and 500 hPa are also in agreement with the  
508 NCEP data except for those in the Qinghai-Tibet Plateau (Figure 9b and c). For the wind field at  
509 850 hPa, the model performs well in the simulation of wind direction, wind speed and wind field  
510 structure in the wintertime of East Asia (Figure 9d). In a word, the modeling results of RegCCMS  
511 show good correlation with the observations, suggesting that RegCCMS is able to capture and  
512 reproduce the features of meteorological fields in different monsoon years.

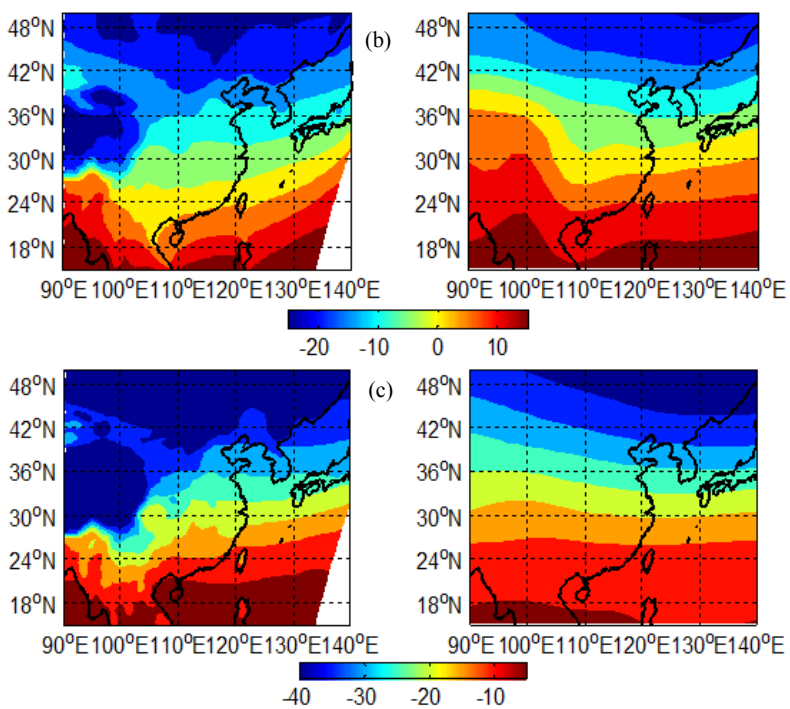
513

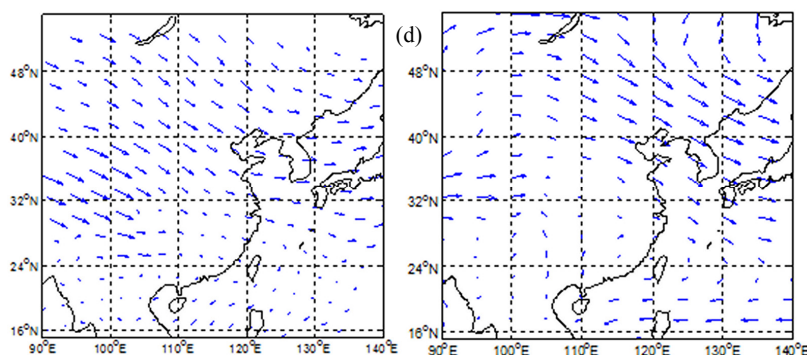


514



515

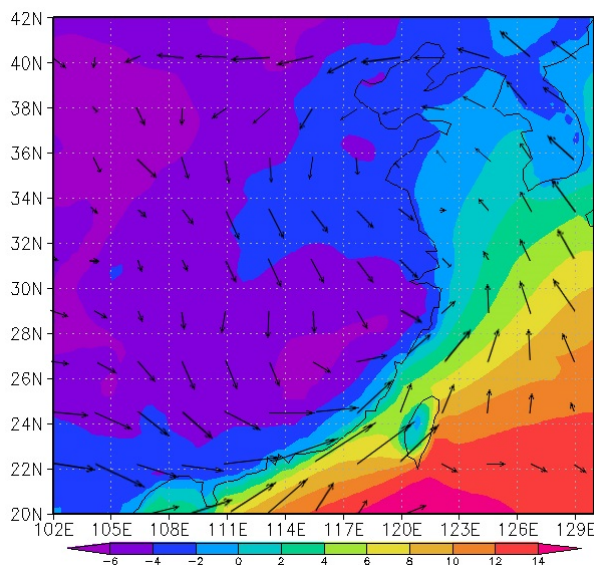




516  
517 **Figure 9. Numerical simulation (left) and observation (right) of meteorological fields, including (a) surface**  
518 **air pressure (unit: hPa); (b) 850 hPa temperature (unit: °C); (c) 500 hPa temperature (unit: °C) and (d) 850**  
519 **hPa wind field (unit: m s<sup>-1</sup>).**

520

521 Figure 10 provides the simulated differences in the distribution of meteorological factors  
522 between the strong and the weak EAWM years, including air temperature at surface and wind field  
523 at 850 hPa. For the wind field at 850 hPa, there is evident cyclonic circulation and northerly air  
524 stream in East China. As a result, the existing northerly wind anomaly is conducive to transport  
525 more cold air masses from the north to the south. Thus, there is a more obvious negative  
526 temperature anomaly in the mainland of East Asia in the strong EAWM years than in the weak  
527 EAWM years. The change areas of air temperature are in agreement with the changes of  
528 atmospheric circulation, which further proves that much stronger northerly wind can result in the  
529 southward invasion of cold air masses and the drop of air temperature in the strong EAWM years.  
530 The above findings from the modeling results coincide with those from the observational data  
531 analysis in Section 3.3, implying that RegCCMS performs well in the simulations for the anomaly  
532 of meteorological fields in the strong and the weak EAWM years.



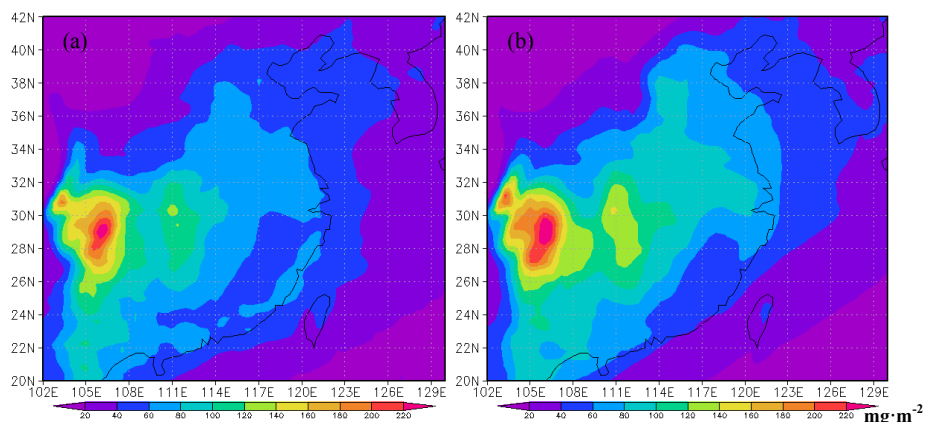
533

534 **Figure 10. Simulated differences in the distribution of meteorological factors between the strong and the**  
535 **weak EAWM years, including surface air temperature (unit: K) with 850 hPa wind field.**

536

537 Figure 11 exhibits the multi-year average aerosol column content in the strong and the weak  
538 EAWM years, which is simulated by RegCCMS. The column content of aerosol is calculated from  
539 surface to the model top. The simulated high values of aerosol loading occur in SCB, Central  
540 China and the coastal areas of East China. Meanwhile, low aerosol loading can be found in the  
541 coastal areas of the provinces of Fujian and Guangdong. The simulated distribution pattern is  
542 generally consistent with that achieved from the satellite observation (Figure 3 and 8). However,  
543 the modeling results do not well catch the maximum values of AOD observed around Bohai Bay  
544 and the coastal areas of YRD. This bias may be attributed to the fact that AOD is not only  
545 correlated with the concentration of aerosol but also affected by moisture. In all, even though the  
546 modeling results and the observation AOD differ in units, it still can be found that RegCCMS well  
547 explains the overall spatial distribution features of wintertime aerosol loading.

548



549

550 **Figure 11. Simulated multiyear mean aerosol column contents in (a) the strong EAWM years and (b) the**  
551 **weak EAWM years by RegCCMS. The column content of aerosol is calculated from surface to the model**  
552 **top.**

553

#### 554 4.2 Effects of strong and weak EAWM on the distribution of aerosols

555 As shown in Figure 11, there is no obvious difference in the aerosol spatial distribution  
556 between the strong and the weak EAWM years. The highest aerosol loading generally occurs in  
557 SCB. However, there still exists some difference. Both the area coverage of high values and the  
558 intensity of aerosol loading are larger in the weak EAWM years, with aerosol column content  
559 reaching high value as  $200 \text{ mg}\cdot\text{m}^{-2}$  and covering the area of  $104^{\circ}\text{E}-107^{\circ}\text{E}$  and  $27^{\circ}\text{N}-30^{\circ}\text{N}$  (Figure  
560 11b). For the strong EAWM years, the high values (higher than  $200 \text{ mg}\cdot\text{m}^{-2}$ ) are limited to the area  
561 of  $106^{\circ}\text{E}-107^{\circ}\text{E}$  and  $28^{\circ}\text{N}-29^{\circ}\text{N}$  (Figure 11a). The result is the same for the differences in regions  
562 with secondary high value. For the area of  $110^{\circ}\text{E}-113^{\circ}\text{E}$  and  $27^{\circ}\text{N}-32^{\circ}\text{N}$ , the aerosol column  
563 content ranges from 140 to  $160 \text{ mg}\cdot\text{m}^{-2}$  in the weak EAWM years, while the value is lower than  
564  $140 \text{ mg}\cdot\text{m}^{-2}$  in the strong EAWM years.

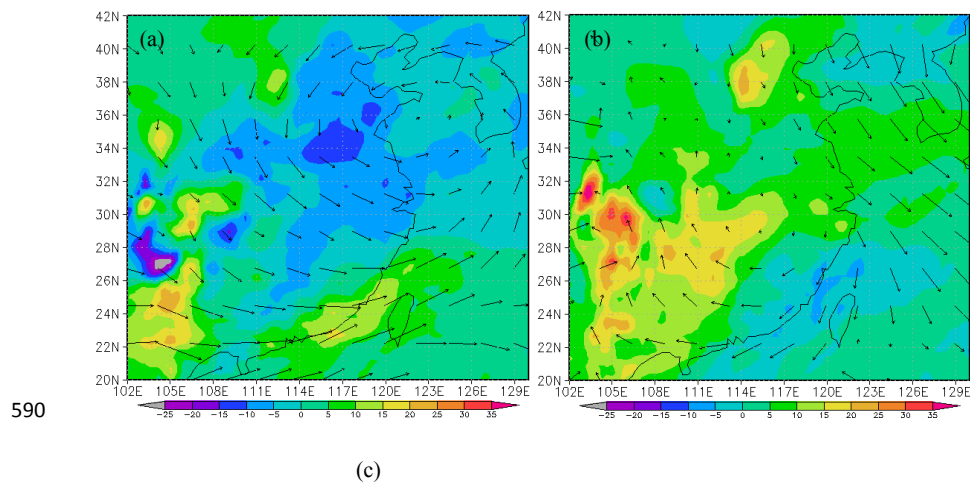
565 Furthermore, Figure 12a and b demonstrate the anomaly of aerosol column content and 850  
566 hPa wind field in the strong and the weak EAWM years, which greatly differ in the spatial  
567 distribution. As shown in Figure 12a, in the strong EAWM years, there is a negative anomaly in  
568 the area east to  $110^{\circ}\text{E}$  and north to  $28^{\circ}\text{N}$ , with the maximum reduction over  $-10 \text{ mg}\cdot\text{m}^{-2}$ . In  
569 contrast, there is a positive anomaly in the weak EAWM years for the same area, with the  
570 maximum increment over  $20 \text{ mg}\cdot\text{m}^{-2}$ . In addition, in the strong (weak) years, there is a negative  
571 (positive) anomaly in the region of  $26^{\circ}\text{N}-30^{\circ}\text{N}$  near SCB, with the maximum change value over

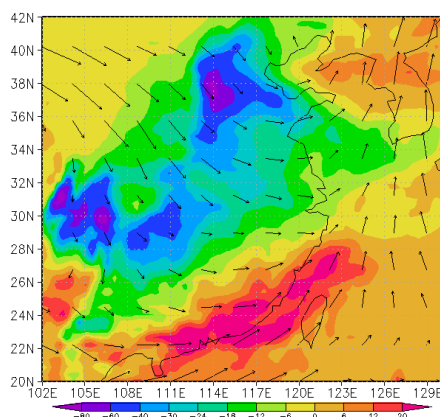


572  $-25$  (30)  $\text{mg}\cdot\text{m}^{-2}$ . As to the wind anomaly at 850 hPa, it can be found that there are a northerly  
573 wind anomaly and an increase in the component of north wind in the strong EAWM years, which  
574 should be linked with the effects of cyclonic circulation over East Asia. On the contrary, East Asia  
575 is influenced by the anticyclonic circulation in the weak EAWM years. There appears a south  
576 wind anomaly and a weaker northerly wind than those in normal years.

577 Figure 12c shows the difference in the distribution of aerosol column content as well as the  
578 wind at 850 hPa between the strong and the weak EAWM years. It appears that the northwest  
579 wind in the area north to  $28^{\circ}\text{N}$  is stronger in the strong EAWM years than in the weak EAWM  
580 years, which helps to transport more aerosols from the north to the south. In consequence, the  
581 decrease of aerosol loading can be found in most land areas of East Asia, with the highest  
582 decrement over  $-60$   $\text{mg}\cdot\text{m}^{-2}$  in North China and SCB in the strong EAWM years. Meanwhile, the  
583 west wind in the area south to  $28^{\circ}\text{N}$  is strong as well, which can further transport aerosols to the  
584 coastal areas in the south. Thus, the synthetic impacts of the north and the west wind cause the  
585 significant increases of aerosols in the coastal areas of Fujian, Guangdong and Guangxi, with the  
586 typical increment over  $25$   $\text{mg}\cdot\text{m}^{-2}$ . This driving effect of wind on the distribution of aerosols  
587 results in the higher AOD value in the south and lower in the north in the strong EAWM years,  
588 which has been displayed in Figure 8.

589





591

592 **Figure 12. Simulated aerosol column content in the strong and the weak EAWM years, including the aerosol**  
593 **column content anomaly and the 850hPa wind anomaly in (a) the strong and (b) the weak EAWM years,**  
594 **and (c) the difference in aerosol column content and 850 hPa wind between the strong and the weak EAWM**  
595 **years (aerosol column content of weak years subtracted from that of strong years).**

596

597 Figure 13 illustrates the aerosol concentration anomalies at surface, 850 hPa and 500 hPa in  
598 the strong and the weak EAWM years, which are calculated by the aerosol concentrations at the  
599 corresponding altitude subtracting from the multi-year average values. As shown in Figure 13a and  
600 b, there is an obvious negative anomaly at surface over East Asia in the strong EAWM years, with  
601 the relatively high decreases in the North China Plain and the highest reduction over  $-23 \mu\text{g}\cdot\text{m}^{-3}$  in  
602 BTH. In the weak EAWM years, there is a positive anomaly in the east of East Asia instead, with  
603 the maximum increment of  $35 \mu\text{g}\cdot\text{m}^{-3}$ . As for the wind field anomaly at surface, there is a stronger  
604 northerly wind over East Asian continent in the strong EAWM years than in normal years  
605 (Figure 13a). This wind anomaly in the strong EAWM years may help to reduce the aerosol  
606 column content by carrying more aerosols from the inland to the sea areas in the southeast of East  
607 Asia. Worthy of note is that there is a relatively larger positive anomaly covering the area of  
608  $104^{\circ}\text{E}\text{-}106^{\circ}\text{E}$ ,  $26^{\circ}\text{N}\text{-}28^{\circ}\text{N}$ , which should be related to the east wind anomaly in this region.  
609 However, in the weak EAWM years, the surface wind slows down, hindering the outward  
610 transport of aerosols and resulting in much more accumulation of aerosols on the land (Figure  
611 13b).

612 As for the changes at 850 hPa, there is a negative anomaly of aerosol concentration in the  
613 North China Plain and the reaches of Yangtze River while a positive anomaly in the areas north to  
614  $26^{\circ}\text{N}$  in the strong EAWM years. As shown in Figure 13c, this change pattern of aerosol

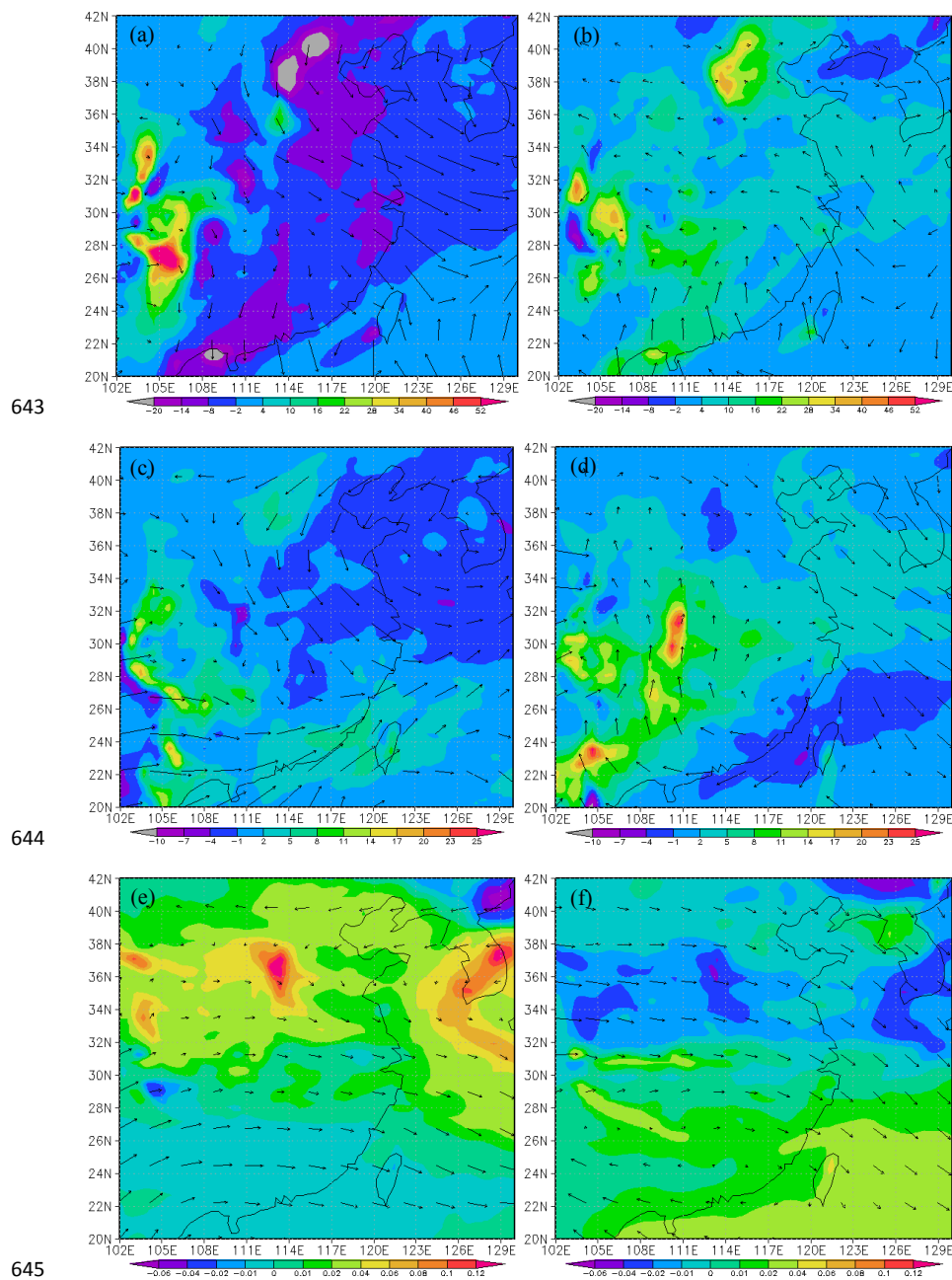


615 distribution should be attributed to the positive anomaly of the northerly wind in most land areas  
616 of East Asian continent. In the weak EAWM years, however, the mainland of East Asian continent  
617 is affected by anticyclonic circulation (Figure 13d). Consequently, there appears a positive aerosol  
618 concentration anomaly in Southwest China, Central China and the Middle-Lower reaches of  
619 Yangtze River. Meanwhile, a negative anomaly occurs in the coastal areas of Fujian and  
620 Guangdong provinces. The region with the biggest difference covers the area of 109°E-111°E,  
621 29°N-32°N, with the decrement (increment) of -10 (23)  $\mu\text{g}\cdot\text{m}^{-3}$  in the strong (weak) EAWM years.

622 Affected by the different changes of monsoon circulation at different altitude, the change  
623 patterns of aerosol and wind at 500 hPa are different from those in lower troposphere. As shown in  
624 Figure 13e, there are stronger northeast wind in the area north to 39 °N and stronger southwest  
625 wind in the area south to 30 °N in the strong EAWM years. Thus, more aerosols accumulate in the  
626 areas between 30°N and 39°N, and thereby there is a positive aerosol concentration anomaly. On  
627 the contrary, there is stronger northwest wind in the mainland of East Asian continent in the weak  
628 EAWM years, which results in a negative aerosol concentration anomaly north to 30°N and a  
629 positive anomaly south to 30°N.

630 To sum up, in the lower troposphere, there is enhanced horizontal wind in the strong EAWM  
631 years, which transports more aerosols to the southeast coastal areas and reduces aerosol  
632 concentrations on the land. However, the aerosols cannot be transported outward in the weak  
633 EAWM years and accumulate around the source areas, increasing the aerosol concentrations in the  
634 mainland of East Asia than those in normal years. The change pattern of aerosol concentrations is  
635 different at 500hPa, which is related with the different change pattern of meteorological fields  
636 affected by the upper part of EAWM circulation. The bigger difference in aerosol concentrations  
637 between the strong and the weak EAWM years occurs in lower troposphere. The changes of  
638 aerosols range from -14 to 30  $\mu\text{g}\cdot\text{m}^{-3}$ , -10 to 23  $\mu\text{g}\cdot\text{m}^{-3}$ , and -0.06 to 0.14  $\mu\text{g}\cdot\text{m}^{-3}$  at surface, 850  
639 hPa, and 500 hPa, respectively. Thus, the change pattern of AOD (or simulated aerosol column  
640 content) in different EAWM years is mainly decided by the change of aerosols in lower  
641 troposphere.

642



646 **Figure 13.** The simulated anomaly of wintertime aerosol concentration and wind field in the strong EAWM  
647 years (a, c and e) and the weak EAWM years (b, d and f) at surface (a and b), 850hPa(c and d), and 500hPa  
648 (e and f) (unit:  $\mu\text{g}\cdot\text{m}^{-3}$ ).

649

650 **5. Conclusion**



651 This paper investigates the impacts of EAWM on the distribution of wintertime aerosol in  
652 East Asia on the basis of observational data analysis and numerical simulations. MODIS/AOD is  
653 used to analyze the spatial distribution and long-term variation trends of aerosols over East Asia.  
654 The EAWM index identified by the characteristics of circulation is adopted to study the long-term  
655 variation of EAWM. The different characteristics of meteorological fields in the strong and the  
656 weak EAWM years are analyzed by using the NCEP reanalysis data. Combined the results from  
657 observations and RegCCMS simulations, the differences in distribution anomaly for aerosols  
658 between strong and weak EAWM years, and the potential transport effects of monsoon circulation  
659 are discussed. The main conclusions are as follows.

660 (1) There exists an increase trend in wintertime AOD over East Asia, which shows obvious  
661 inter-annual variation characteristics with the maximum value of 0.44 in 2007 and the minimum  
662 value of 0.36 in 2001. In winter, high AOD values mainly occur over SCB, the North China Plain  
663 and most of the Middle-Lower reaches of Yangtze River. Moreover, there are obvious increases of  
664 AOD in these regions.

665 (2) With the aid of the EAWM index, it can be summarized that there are 9 strong EAWM  
666 years (1979, 1980, 1982-1985, 1996, 2001 and 2010) and 13 weak EAWM years (1986-1989,  
667 1997, 1998, 2002, 2005-2006, 2008, and 2012-2014) during the period from 1979 to 2014. The  
668 intensity of winter monsoon is stronger before 1986 and gets weakened since 1986. The  
669 meteorological conditions differ in different EAWM years. In the strong EAWM years, the  
670 sea-land pressure contrast gets increased, the East Asian trough gets strengthened, and the  
671 northerly wind anomaly dominates over East Asia. The stronger wind transports more cold air  
672 masses southward and causes the air temperature drop in the mainland of East Asia. The change  
673 patterns of meteorological factors are just the opposite of those in the weak EAWM years.

674 (3) Though higher aerosol loading in winter is largely ascribed to the huge emission  
675 generated by human activities, the EAWM circulation can change the distribution of aerosols as  
676 well. The northerly wind speeds up over East Asia in the strong EAWM years and transports  
677 aerosols southward, resulting in AOD higher in the south and lower in the north of East Asia. In  
678 contrast, in the weak EAWM years, the northerly wind slows down and allows more aerosols to  
679 accumulate in the North China Plain, resulting in AOD higher in the north and lower in the south.  
680 The long-term weakening trend of EAWM may potentially increase the aerosol loading over YRD,



681 BTH and SCB, while causes the decrease of AOD over PRD.

682 (4) It is further confirmed by numerical simulation that the stronger (weaker) northerly wind  
683 transports more (less) aerosols southward and there appears a negative (positive) aerosol column  
684 content anomaly in mainland China in the strong (weak) EAWM years. The difference in aerosol  
685 column content between the strong and the weak EAWM years ranges from  $-80 \text{ mg}\cdot\text{m}^{-2}$  to  
686  $25 \text{ mg}\cdot\text{m}^{-2}$ . The change pattern of aerosol concentrations in lower troposphere is different from that  
687 at 500 hPa, which is related with the different change pattern of meteorological fields in EAWM  
688 circulation at different altitude. The changes of aerosols range from  $-14$  to  $30 \text{ }\mu\text{g}\cdot\text{m}^{-3}$ ,  $-10$  to  
689  $23 \text{ }\mu\text{g}\cdot\text{m}^{-3}$  and  $-0.06$  to  $0.14 \text{ }\mu\text{g}\cdot\text{m}^{-3}$  at surface, 850 hPa and 500 hPa, respectively. The change  
690 pattern of aerosol column content in different EAWM years is mainly decided by the change of  
691 aerosols in lower troposphere.

692 It has been proved that the variations of EAWM can directly affect the transport, diffusion,  
693 deposition and chemical reaction processes of aerosols. This paper is only concerned about the  
694 effects of strong and weak EAWM on the transport of aerosols. Therefore, future researches  
695 considering the effects of EAWM on other processes of aerosols are needed to deepen the  
696 discussion. Moreover, the data for aerosols in various types with high resolution have been  
697 available, thus more specific studies about effects of EAWM on different kinds of aerosols should  
698 be strengthened in the future as well.

699

#### 700 **Acknowledgments**

701 This work was supported by the National Natural Science Foundation of China (41475122,  
702 91544230, 41621005), the National Key Research and Development Program of China  
703 (2016YFA0602104), the open research fund of Chongqing Meteorological Bureau (KFJJ-201607),  
704 and the Fundamental Research Funds for the Central Universities. The authors would like to thank  
705 the anonymous reviewers for their constructive and precious comments on this manuscript.

706

#### 707 **References**

708 Albrecht, B. A.: Aerosols, Cloud Microphysics, And Fractional Cloudiness, *Science*, 245,  
709 1227-1230, 1989.  
710 Allen, R. J., Norris, J. R., and Kovilakam, M.: Influence of anthropogenic aerosols and the Pacific  
711 Decadal Oscillation on tropical belt width, *Nat Geosci*, 7, 270-274, [10.1038/ngeo2091](https://doi.org/10.1038/ngeo2091), 2014.



- 712 Bian, J., and Yan, R.: Tropospheric Pollutant Transport to the Stratosphere by Asian Summer  
713 Monsoon, *Chinese Journal of Atmospheric Sciences*, 35, 897-902, 2011.
- 714 Bollasina, M. A., Ming, Y., and Ramaswamy, V.: Anthropogenic Aerosols and the Weakening of  
715 the South Asian Summer Monsoon, *Science*, 334, 502-505, 10.1126/science.1204994, 2011.
- 716 Bollasina, M. A., Ming, Y., Ramaswamy, V., Schwarzkopf, M. D., and Naik, V.: Contribution of  
717 local and remote anthropogenic aerosols to the twentieth century weakening of the South Asian  
718 Monsoon, *Geophys Res Lett*, 41, 680-687, 10.1002/2013GL058183, 2014.
- 719 Chen, Y., Xie, S. D., Luo, B., and Zhai, C. Z.: Characteristics and origins of carbonaceous aerosol  
720 in the Sichuan Basin, China, *Atmos Environ*, 94, 215-223, 2014.
- 721 Chen, H., and Wang, H.: Haze Days in North China and the associated atmospheric circulations  
722 based on daily visibility data from 1960 to 2012, *Journal of Geophysical Research*  
723 *Atmospheres*, 120, 5895-5909, 2015.
- 724 Chu, D. A., Kaufman, Y. J., Ichoku, C., Remer, L. A., Tanre, D., and Holben, B. N.: Validation of  
725 MODIS aerosol optical depth retrieval over land, *Geophys Res Lett*, 29, 2002.
- 726 Dickinson, R. E.: Biosphere-atmosphere transfer scheme(BATS) version IE as coupled to the  
727 NCARcommunity climate model, NCAR Tech .Note NCAR/ TN\_387\_STR, National Center  
728 for Atmospheric Research, Boulder , Colorado, 1993.
- 729 Ding, A. J., Fu, C. B., Yang, X. Q., Sun, J. N., Petaja, T., Kerminen, V. M., Wang, T., Xie, Y.,  
730 Herrmann, E., Zheng, L. F., Nie, W., Liu, Q., Wei, X. L., and Kulmala, M.: Intense  
731 atmospheric pollution modifies weather: a case of mixed biomass burning with fossil fuel  
732 combustion pollution in eastern China, *Atmos Chem Phys*, 13, 10545-10554, 2013.
- 733 Ding, A. J., Huang, X., Nie, W., Sun, J. N., Kerminen, V. M., Petaja, T., Su, H., Cheng, Y. F.,  
734 Yang, X. Q., Wang, M. H., Chi, X. G., Wang, J. P., Virkkula, A., Guo, W. D., Yuan, J., Wang,  
735 S. Y., Zhang, R. J., Wu, Y. F., Song, Y., Zhu, T., Zilitinkevich, S., Kulmala, M., and Fu, C. B.:  
736 Enhanced haze pollution by black carbon in megacities in China, *Geophys Res Lett*, 43,  
737 2873-2879, 2016.
- 738 Fan, J., Leung, L. R., Li, Z., Morrison, H., Chen, H., Zhou, Y., Qian, Y., and Wang, Y.: Aerosol  
739 impacts on clouds and precipitation in eastern China: Results from bin and bulk microphysics,  
740 *Journal of Geophysical Research: Atmospheres*, 117, 2012.
- 741 Fan, J., Leung, L. R., Rosenfeld, D., Chen, Q., Li, Z., Zhang, J., and Yan, H.: Microphysical  
742 effects determine macrophysical response for aerosol impacts on deep convective clouds,  
743 *Proceedings of the National Academy of Sciences*, 110, E4581-E4590, 2013.
- 744 Fu, R., Hu, Y., Wright, J. S., Jiang, J. H., Dickinson, R. E., Chen, M., Filipiak, M., Read, W. G.,  
745 Waters, J. W., and Wu, D. L.: From the Cover: Short circuit of water vapor and polluted air to  
746 the global stratosphere by convective transport over the Tibetan Plateau, *Proc Natl Acad Sci U*  
747 *S A*, 103, 5664-5669, 2006.
- 748 Ganguly, D., Rasch, P. J., Wang, H., and Yoon, J. H.: Climate response of the South Asian  
749 monsoon system to anthropogenic aerosols, *Journal of Geophysical Research: Atmospheres*,  
750 117, 2012.
- 751 Giorgi, F., Bi, X. Q., and Qian, Y.: Indirect vs. direct effects of anthropogenic sulfate on the  
752 climate of East Asia as simulated with a regional coupled climate-chemistry/aerosol model,  
753 *Climatic Change*, 58, 345-376, 2003.
- 754 Giorgi, F., Bi, X., and Pal, J. S.: Mean, interannual variability and trends in a regional climate  
755 change experiment over Europe. I. Present-day climate (1961-1990), *Clim Dynam*, 22,



- 756 733-756, 2004a.
- 757 Giorgi, F., Bi, X. Q., and Pal, J.: Mean, interannual variability and trends in a regional climate  
758 change experiment over Europe. II: climate change scenarios (2071-2100), *Clim Dynam*, 23,  
759 839-858, 2004b.
- 760 Grell, G. A., and Devenyi, D.: A generalized approach to parameterizing convection combining  
761 ensemble and data assimilation techniques, *Geophys Res Lett*, 29, 2002.
- 762 Guo, S., Hu, M., Zamora, M. L., Peng, J. F., Shang, D. J., Zheng, J., Du, Z. F., Wu, Z., Shao, M.,  
763 Zeng, L. M., Molina, M. J., and Zhang, R. Y.: Elucidating severe urban haze formation in  
764 China, *P Natl Acad Sci USA*, 111, 17373-17378, 2014.
- 765 Holtzlag, A. A. M., and Boville, B. A.: Local Versus Nonlocal Boundary-Layer Diffusion In a  
766 Global Climate Model, *J Climate*, 6, 1825-1842, 1993.
- 767 Isaksen, I. S. A., Granier, C., Myhre, G., Berntsen, T. K., Dalsoren, S. B., Gauss, M., Klimont, Z.,  
768 Benestad, R., Bousquet, P., Collins, W., Cox, T., Eyring, V., Fowler, D., Fuzzi, S., Jockel, P.,  
769 Laj, P., Lohmann, U., Maione, M., Monks, P., Prevo, A. S. H., Raes, F., Richter, A., Rognerud,  
770 B., Schulz, M., Shindell, D., Stevenson, D. S., Storelvmo, T., Wang, W. C., van Weele, M.,  
771 Wild, M., and Wuebbles, D.: Atmospheric composition change: Climate-Chemistry  
772 interactions, *Atmos Environ*, 43, 5138-5192, 2009.
- 773 Jacob, D. J., and Winner, D. A.: Effect of climate change on air quality, *Atmos Environ*, 43, 51-63,  
774 2009.
- 775 Jacobson, M. Z., and Kaufman, Y. J.: Wind reduction by aerosol particles, *Geophys Res Lett*, 33,  
776 2006.
- 777 Jhun, J. G., and Lee, E. J.: A new East Asian winter monsoon index and associated characteristics  
778 of the winter monsoon, *J Climate*, 17, 711-726, 2004.
- 779 Kiehl, J. T., Hack, J. J., Bonan, G. B., Boville, B. A., Briegleb, B. P., Williamson, D. L., Rasch, P.  
780 J.: Description of the NCAR Community Climate Model (CCM3). NCAR Tech Note  
781 NCAR/TN-420+STR, Nat. Cent. for Atmos. Res., Boulder, CO, 152, 1996
- 782 Konwar, M., Mahes Kumar, R., Kulkarni, J., Freud, E., Goswami, B., and Rosenfeld, D.: Aerosol  
783 control on depth of warm rain in convective clouds, *Journal of Geophysical Research:  
784 Atmospheres*, 117, 2012.
- 785 Lau, K., Kim, M., and Kim, K.: Asian summer monsoon anomalies induced by aerosol direct  
786 forcing: the role of the Tibetan Plateau, *Clim Dynam*, 26, 855-864, 2006.
- 787 Li, Z., Xia, X., Cribb, M., Mi, W., Holben, B., Wang, P., Chen, H., Tsay, S. C., Eck, T., and Zhao,  
788 F.: Aerosol optical properties and their radiative effects in northern China, *Journal of  
789 Geophysical Research: Atmospheres*, 112, 2007.
- 790 Li, S., Wang, T. J., Zhuang, B. L., and Han, Y.: Indirect radiative forcing and climatic effect of the  
791 anthropogenic nitrate aerosol on regional climate of China, *Adv Atmos Sci*, 26, 543-552, 2009.
- 792 Li, Z. Q., Lee, K. H., Wang, Y. S., Xin, J. Y., and Hao, W. M.: First observation-based estimates  
793 of cloud-free aerosol radiative forcing across China, *J Geophys Res-Atmos*, 115, 2010.
- 794 Li, Z. Q., Li, C., Chen, H., Tsay, S. C., Holben, B., Huang, J., Li, B., Maring, H., Qian, Y., Shi, G.,  
795 Xia, X., Yin, Y., Zheng, Y., and Zhuang, G.: East Asian Studies of Tropospheric Aerosols and  
796 their Impact on Regional Climate (EAST-AIRC): An overview, *J Geophys Res-Atmos*, 116,  
797 2011.
- 798 Li, J. W., Han, Z. W.: Numerical simulation of the seasonal variation of aerosol optical depth over  
799 eastern China, *Journal of Remote Sensing*, 20, 205-215, 10.11834/jrs.20165106, 2016.



- 800 Li, Q., Zhang, R. H., and Wang, Y.: Interannual variation of the wintertime fog-haze days across  
801 central and eastern China and its relation with East Asian winter monsoon, *Int J Climatol*, 36,  
802 346-354, 2016a.
- 803 Li, S., Wang, T. J., Solmon, F., Zhuang, B. L., Wu, H., Xie, M., Han, Y., and Wang, X. M.:  
804 Impact of aerosols on regional climate in southern and northern China during strong/weak East  
805 Asian summer monsoon years, *J Geophys Res-Atmos*, 121, 4069-4081,  
806 10.1002/2015JD023892, 2016b.
- 807 Li, Z. Q., Lau, W. K. M., Ramanathan, V., Wu, G., Ding, Y., Manoj, M. G., Liu, J., Qian, Y., Li,  
808 J., Zhou, T., Fan, J., Rosenfeld, D., Ming, Y., Wang, Y., Huang, J., Wang, B., Xu, X., Lee, S.  
809 S., Cribb, M., Zhang, F., Yang, X., Zhao, C., Takemura, T., Wang, K., Xia, X., Yin, Y., Zhang,  
810 H., Guo, J., Zhai, P. M., Sugimoto, N., Babu, S. S., and Brasseur, G. P.: Aerosol and monsoon  
811 climate interactions over Asia, *Rev Geophys*, 54, 866-929, 10.1002/2015RG000500, 2016c.
- 812 Liu, H., Jacob, D. J., Bey, I., Yantosca, R. M., Duncan, B. N., and Sachse, G. W.: Transport  
813 pathways for Asian pollution outflow over the Pacific: Interannual and seasonal variations,  
814 *Journal of Geophysical Research Atmospheres*, 108, 1445-1459, 2003.
- 815 Liu, X., Yan, L., Yang, P., Yin, Z. Y., and North, G. R.: Influence of Indian Summer Monsoon on  
816 Aerosol Loading in East Asia, *Journal of Applied Meteorology & Climatology*, 50, 523-533,  
817 2011.
- 818 Liu, L., Li, Z., Yang, X., Gong, H., Li, C., and Xiong, A.: The long - term trend in the diurnal  
819 temperature range over Asia and its natural and anthropogenic causes, *Journal of Geophysical  
820 Research: Atmospheres*, 121, 3519-3533, 2016.
- 821 Manoj, M. G., Devara, P. C. S., Joseph, S., and Sahai, A. K.: Aerosol indirect effect during the  
822 aberrant Indian Summer Monsoon breaks of 2009, *Atmos Environ*, 60, 153-163, 2012.
- 823 Mu, M., and Zhang, R. H.: Addressing the issue of fog and haze: A promising perspective from  
824 meteorological science and technology, *Science China Earth Sciences*, 57, 1-2, 2014.
- 825 Nair, S., Sanjay, J., Pandithurai, G., Mahes Kumar, R., and Kulkarni, J.: On the parameterization of  
826 cloud droplet effective radius using CAIPEEX aircraft observations for warm clouds in India,  
827 *Atmospheric Research*, 108, 104-114, 2012.
- 828 Nakajima, T., Sekiguchi, M., Takemura, T., Uno, I., Higurashi, A., Kim, D., BYUNG, J. S., Oh,  
829 S.-N., Nakajima, T. Y., and Ohta, S.: Significance of direct and indirect radiative forcings of  
830 aerosols in the East China Sea region: Characterization of Asian aerosols and their radiative  
831 impacts on climate, *Journal of geophysical research*, 108, ACE26. 21-ACE26. 16, 2003.
- 832 Nakamura, H., Izumi, T., and Sampe, T.: Interannual and decadal modulations recently observed  
833 in the Pacific storm track activity and east Asian winter monsoon, *J Climate*, 15, 1855-1874,  
834 2002.
- 835 Nenes, A., Pandis, S. N., and Pilinis, C.: ISORROPIA: A new thermodynamic equilibrium model  
836 for multiphase multicomponent inorganic aerosols, *Aquat Geochem*, 4, 123-152, Doi  
837 10.1023/A:1009604003981, 1998.
- 838 Niu, F., Li, Z., Li, C., Lee, K. H., and Wang, M.: Increase of wintertime fog in China: Potential  
839 impacts of weakening of the Eastern Asian monsoon circulation and increasing aerosol loading,  
840 *Journal of Geophysical Research: Atmospheres*, 115, 2010.
- 841 Pal, J. S., Giorgi, F., Bi, X. Q., Elguindi, N., Solmon, F., Gao, X. J., Rauscher, S. A., Francisco, R.,  
842 Zakey, A., Winter, J., Ashfaq, M., Syed, F. S., Bell, J. L., Diffenbaugh, N. S., Karmacharya, J.,  
843 Konare, A., Martinez, D., da Rocha, R. P., Sloan, L. C., and Steiner, A. L.: Regional climate



- 844 modeling for the developing world - The ICTP RegCM3 and RegCNET, *B Am Meteorol Soc*,  
845 88, 1395-+, [10.1175/Bams-88-9-1395](https://doi.org/10.1175/Bams-88-9-1395), 2007.
- 846 Press, W. H., Teukolsky, S. A., Vetterling, W. T., Flannery, B. P.: *Numerical Recipes in C. The*  
847 *Art of Scientific Computing*, 2nd ed., Cambridge Univ. Press, New York, 1992.
- 848 Qian, Y., Gong, D., Fan, J., Leung, L. R., Bennartz, R., Chen, D., and Wang, W.: Heavy pollution  
849 suppresses light rain in China: Observations and modeling, *Journal of Geophysical Research:*  
850 *Atmospheres*, 114, 2009.
- 851 Quan, J. N., Tie, X. X., Zhang, Q., Liu, Q., Li, X., Gao, Y., and Zhao, D. L.: Characteristics of  
852 heavy aerosol pollution during the 2012-2013 winter in Beijing, China, *Atmos Environ*, 88,  
853 83-89, 2014.
- 854 Ramanathan, V., Crutzen, P. J., Kiehl, J. T., and Rosenfeld, D.: Atmosphere - Aerosols, climate,  
855 and the hydrological cycle, *Science*, 294, 2119-2124, 2001a.
- 856 Ramanathan, V., Crutzen, P. J., Lelieveld, J., Mitra, A. P., Althausen, D., Anderson, J., Andreae,  
857 M. O., Cantrell, W., Cass, G. R., and Chung, C. E.: Indian Ocean Experiment: An integrated  
858 analysis of the climate forcing and effects of the great Indo - Asian haze, *Journal of*  
859 *Geophysical Research Atmospheres*, 106, 28371-28398, 2001b.
- 860 Randel, W. J., Park, M. J., Emmons, L., Kinnison, D., Bernath, P., Walker, K. A., Boone, C., and  
861 Pumphrey, H.: Asian monsoon transport of pollution to the stratosphere, *Science*, 328, 611,  
862 2010.
- 863 Rosenfeld, D.: Suppression of rain and snow by urban and industrial air pollution, *Science*, 287,  
864 1793-1796, 2000.
- 865 Rosenfeld, D., Lohmann, U., Raga, G. B., O'Dowd, C. D., Kulmala, M., Fuzzi, S., Reissell, A.,  
866 and Andreae, M. O.: Flood or drought: How do aerosols affect precipitation?, *Science*, 321,  
867 1309-1313, 2008.
- 868 Shao, P. C., Li, D. L.: Classification and comparison of east Asian winter monsoon indices,  
869 *Journal of the Meteorological Sciences*, 32, 226-235, [10.3969/2012jms.0018](https://doi.org/10.3969/2012jms.0018), 2012.
- 870 Smolarkiewicz, P. K.: A Fully Multidimensional Positive Definite Advection Transport Algorithm  
871 with Small Implicit Diffusion, *J Comput Phys*, 54, 325-362, [Doi 10.1016/0021-9991\(84\)90121-9](https://doi.org/10.1016/0021-9991(84)90121-9), 1984.
- 872 Song, F., Zhou, T., and Qian, Y.: Responses of East Asian summer monsoon to natural and  
873 anthropogenic forcings in the 17 latest CMIP5 models, *Geophys Res Lett*, 41, 596-603, 2014.
- 874 Tang, J., Wang, P., Mickley, L. J., Xia, X., Liao, H., Yue, X., Sun, L., and Xia, J.: Positive  
875 relationship between liquid cloud droplet effective radius and aerosol optical depth over  
876 Eastern China from satellite data, *Atmos Environ*, 84, 244-253, 2014.
- 877 Tao, J. H., Zhang, M. G., Chen, L. F., Wang, Z. F., Su, L., Ge, C., Han, X., and Zou, M. M.: A  
878 method to estimate concentrations of surface-level particulate matter using satellite-based  
879 aerosol optical thickness, *Sci China Earth Sci*, 56, 1422-1433, 2013.
- 880 Twomey, S.: Influence Of Pollution on Shortwave Albedo Of Clouds, *J Atmos Sci*, 34, 1149-1152,  
881 1977.
- 882 von Schneidmesser, E., Monks, P. S., Allan, J. D., Bruhwiler, L., Forster, P., Fowler, D., Lauer,  
883 A., Morgan, W. T., Paasonen, P., Righi, M., Sindelarova, K., and Sutton, M. A.: Chemistry and  
884 the Linkages between Air Quality and Climate Change, *Chem Rev*, 115, 3856-3897, 2015.
- 885 Walmsley, J. L., and Wesely, M. L.: Modification of coded parametrizations of surface resistances  
886 to gaseous dry deposition, *Atmos Environ*, 30, 1181-1188, [Doi 10.1016/0950-0687\(96\)00181-8](https://doi.org/10.1016/0950-0687(96)00181-8)
- 887



- 888 10.1016/1352-2310(95)00403-3, 1996.
- 889 Wang, L. L., Xin, J. Y., Wang, Y. S., Li, Z. Q., Wang, P. C., Liu, G. R., and Wen, T. X.:  
890 Validation of MODIS aerosol products by CSHNET over china, Chinese Sci Bull, 52,  
891 1708-1718, 2007.
- 892 Wang, L., Huang, R. H., Gu, L., Chen, W., and Kang, L. H.: Interdecadal Variations of the East  
893 Asian Winter Monsoon and Their Association with Quasi-Stationary Planetary Wave Activity,  
894 J Climate, 22, 4860-4872, 2009.
- 895 Wang, T. J., Li, S., Shen, Y., Deng, J. J., and Xie, M.: Investigations on direct and indirect effect  
896 of nitrate on temperature and precipitation in China using a regional climate chemistry  
897 modeling system, J Geophys Res-Atmos, 115, 2010.
- 898 Wang, H. J., and He, S. P.: Weakening relationship between East Asian winter monsoon and  
899 ENSO after mid-1970s, Chinese Sci Bull, 57, 3535-3540, 2012.
- 900 Wang, L., and Chen, W.: An Intensity Index for the East Asian Winter Monsoon, J Climate, 27,  
901 2361-2374, 2014.
- 902 Wang, T. J., Zhuang, B. L., Li, S., Liu, J., Xie, M., Yin, C. Q., Zhang, Y., Yuan, C., Zhu, J. L., Ji,  
903 L. Q., and Han, Y.: The interactions between anthropogenic aerosols and the East Asian  
904 summer monsoon using RegCCMS, J Geophys Res-Atmos, 120, 5602-5621, 2015.
- 905 Wu, G. X., Li, Z. Q., Fu, C. B., Zhang, X. Y., Zhang, R. Y., Zhang, R. H., Zhou, T. J., Li, J. P., Li,  
906 J. D., Zhou, D. G., Wu, L., Zhou, L. T., He, B., and Huang, R. H.: Advances in studying  
907 interactions between aerosols and monsoon in China, Sci China Earth Sci, 59, 1-16, 2016.
- 908 Xie, M., Liao, J. B., Wang, T. J., Zhu, K. G., Zhuang, B. L., Han, Y., Li, M. M., and Li, S.:  
909 Modeling of the anthropogenic heat flux and its effect on regional meteorology and air quality  
910 over the Yangtze River Delta region, China, Atmos Chem Phys, 16, 6071-6089,  
911 10.5194/acp-16-6071-2016, 2016.
- 912 Xie, M., Shu, L., Wang, T. J., Liu, Q., Gao, D., Li, S., Zhuang, B. L., Han, Y., Li, M. M., and  
913 Chen, P. L.: Natural emissions under future climate condition and their effects on surface  
914 ozone in the Yangtze River Delta region, China, Atmos Environ, 150, 162-180, 2017.
- 915 Xu, M., Chang, C. P., Fu, C. B., Qi, Y., Robock, A., Robinson, D., and Zhang, H. M.: Steady  
916 decline of east Asian monsoon winds, 1969-2000: Evidence from direct ground measurements  
917 of wind speed, J Geophys Res-Atmos, 111, 2006.
- 918 Yan, H. M., Duan, W., Xiao, Z. N.: A study on relation between East Asian winter monsoon and  
919 climate change during raining season in China, Journal of Tropical Meteorology, 10, 23-33,  
920 2004.
- 921 Yan, L., Liu, X., Yang, P., Yin, Z. Y., and North, G. R.: Study of the Impact of Summer Monsoon  
922 Circulation on Spatial Distribution of Aerosols in East Asia Based on Numerical Simulations,  
923 Journal of Applied Meteorology & Climatology, 50, 2270-2282, 2011.
- 924 Yang, X., Yao, Z., Li, Z., and Fan, T.: Heavy air pollution suppresses summer thunderstorms in  
925 central China, Journal of Atmospheric and Solar-Terrestrial Physics, 95, 28-40, 2013.
- 926 Zhang, R. H.: Relations of water vapor transport from Indian monsoon with that over East Asia  
927 and the summer rainfall in China, Adv Atmos Sci, 18, 1005-1017, 2001.
- 928 Zhang, X. Y., Wang, Y. Q., Zhang, X. C., Guo, W., Niu, T., Gong, S. L., Yin, Y., Zhao, P., Jin, J.  
929 L., and Yu, M.: Aerosol monitoring at multiple locations in China: contributions of EC and  
930 dust to aerosol light absorption, Tellus B, 60, 647-656, 2008.
- 931 Zhang, Q., Streets, D. G., Carmichael, G. R., He, K. B., Huo, H., Kannari, A., Klimont, Z., Park, I.



- 932 S., Reddy, S., Fu, J. S., Chen, D., Duan, L., Lei, Y., Wang, L. T., and Yao, Z. L.: Asian  
933 emissions in 2006 for the NASA INTEX-B mission, *Atmos Chem Phys*, 9, 5131-5153, 2009.
- 934 Zhang, L., Liao, H., and Li, J.: Impacts of Asian summer monsoon on seasonal and interannual  
935 variations of aerosols over eastern China, *Journal of Geophysical Research Atmospheres*, 115,  
936 2232-2232, 2010.
- 937 Zhang, Q., Geng, G. N., Wang, S. W., Richter, A., and He, K. B.: Satellite remote sensing of  
938 changes in NO (x) emissions over China during 1996-2010, *Chinese Sci Bull*, 57, 2857-2864,  
939 2012a.
- 940 Zhang, X. Y., Wang, Y. Q., Niu, T., Zhang, X. C., Gong, S. L., Zhang, Y. M., and Sun, J. Y.:  
941 Atmospheric aerosol compositions in China: spatial/temporal variability, chemical signature,  
942 regional haze distribution and comparisons with global aerosols, *Atmos Chem Phys*, 12,  
943 779-799, 2012b.
- 944 Zhang, X. Y., Sun, J. Y., Wang, Y. Q., Weijun, L. I., Zhang, Q., Wang, W. G., Quan, J. N., Cao,  
945 G. L., Wang, J. Z., and Yang, Y. Q. A.: Factors contributing to haze and fog in China, *Chinese  
946 Journal*, 58, 2013.
- 947 Zhang, R. H., Li, Q., and Zhang, R. N.: Meteorological conditions for the persistent severe fog and  
948 haze event over eastern China in January 2013, *Sci China Earth Sci*, 57, 26-35, 2014.
- 949 Zhao, C., Wang, Y., Yang, Q., Fu, R., Cunnold, D., and Choi, Y.: Impact of East Asian summer  
950 monsoon on the air quality over China: View from space, *Journal of Geophysical Research  
951 Atmospheres*, 115, 1063-1063, 2010.
- 952 Zhao, X. J., Zhao, P. S., Xu, J., Meng, W., Pu, W. W., Dong, F., He, D., and Shi, Q. F.: Analysis  
953 of a winter regional haze event and its formation mechanism in the North China Plain, *Atmos  
954 Chem Phys*, 13, 5685-5696, 2013.
- 955 Zheng, G. J., Duan, F. K., Su, H., Ma, Y. L., Cheng, Y., Zheng, B., Zhang, Q., Huang, T., Kimoto,  
956 T., Chang, D., Poschl, U., Cheng, Y. F., and He, K. B.: Exploring the severe winter haze in  
957 Beijing: the impact of synoptic weather, regional transport and heterogeneous reactions, *Atmos  
958 Chem Phys*, 15, 2969-2983, 2015.
- 959 Zhu, J., Liao, H., and Li, J.: Increases in aerosol concentrations over eastern China due to the  
960 decadal - scale weakening of the East Asian summer monsoon, *Geophys Res Lett*, 39, 9809,  
961 2012.
- 962 Zhuang, B. L., Li, S., Wang, T. J., Deng, J. J., Xie, M., Yin, C. Q., and Zhu, J. L.: Direct radiative  
963 forcing and climate effects of anthropogenic aerosols with different mixing states over China,  
964 *Atmos Environ*, 79, 349-361, 2013a.
- 965 Zhuang, B. L., Liu, Q., Wang, T. J., Yin, C. Q., Li, S., Xie, M., Jiang, F., and Mao, H. T.:  
966 Investigation on semi-direct and indirect climate effects of fossil fuel black carbon aerosol over  
967 China, *Theor Appl Climatol*, 114, 651-672, 2013b.
- 968
- 969